C.P. No. 1111

C.P. No. 1111

MINISTRY OF TECHNOLOGY

AERONAUTICAL RESEARCH COUNCIL

CURRENT PAPERS

Interim Note on Tests with a Wing-Mounted Fan Nacelle with the Fan Jet Simulated by Cold Air Blowing and Alternatively by a Gas Generator Shroud

By

G Pauley

A.R.A. Bedford

LONDON: HER MAJESTY'S STATIONERY OFFICE

1970

PRICE 14s 0d [70p] NET

C.P. No. 1111*
March 1968

INTERIM NOTE ON TESTS WITH A WING MOUNTED FAN NACELLE WITH THE FAN JET SIMULATED BY COLD AIR BLOWING AND ALTERNATIVELY BY A GAS GENERATOR SHROUD

By

G. Pauley
A.R.A. Bedford

SUMMARY

Wind tunnel tests have been made on a simulated high by-pass ratio fan engine mounted close to a wing to determine the interference effects in the Mach-number range $0.6 < M < 0.81$. The nacelle and adjacent wing surfaces were fully pressure plotted and overall force measurements were obtained. Salient features of the results are discussed in this note, but actual nacelle drag increments are not quoted.

Comparison of test data from a free flow nacelle supported by a representative pylon and a "minimum" pylon suggests that the nacelle has a major influence on the local wing flow, whereas it seems likely that a pylon could be designed to have relatively little effect on this flow.

Tests on a nacelle with a cold fan jet exhausting at $H_J/H_o = 1.5$ demonstrated that free flow nacelle effects were amplified by the jet. An attempt at reproducing the jet effects by using a simple gas generator shroud was a complete failure. It is however still possible that now that the fan jet effects are known, a more effective shroud, i.e., extended-cowl nacelle, could be devised.

* Replaces A.R.A. Model Test Note M.28/1 - A.R.C.30 158

CONTENTS

FIGURES

NOTATION

$\frac{A_o}{A_i}$	Mass flow ratio based on highlight area
c	Chord
C_L	Lift coefficient
C_p	Pressure coefficient
C_{pylon}	Pylon chord
C_{wing}	Wing chord
H_J	Jet total pressure
H_o	Free stream total pressure
I/B	Inboard
L_F	Length of fan cowl
L.S.	Lower surface
M	Mach number
O/B	Outboard
R_c	Reynolds number based on local wing chord
R_D	Reynolds number based on fan cowl maximum diameter
U/S	Upper surface
x	Distance from leading edge or highlight
x_G	Distance aft of fan nozzle measured along gas generator cowl
α_b	Wing and fuselage incidence, the nacelle incidence and local wing incidence at the nacelle position = $(\alpha_b - 1^\circ\ 20')$

1. INTRODUCTION

High by-pass ratio fan engines for transport aircraft are currently being designed with diameters about twice as large as those for engines in use at the present day. Consequently the interference drag of the engine installation assumes a greater importance than hitherto. The aim of the tests to be described, was to examine a representative installation of such an engine mounted relatively close to a wing, as required on a low wing airbus-type layout, and in particular to determine whether jet effects would then be significant, and if so whether these could be simulated by an extended fan cowl (i.e. a shrouded gas generator cowl).

The present note has been prepared prior to publication of a complete report, in order that the information should be available to assist in the design of similar models.

2. DESCRIPTION OF MODEL

The nacelle was mounted on an existing HS.681 half-model (fig.1) which had an early wing design based on the DH.129 wing (based on section C). The nacelle was stationed at 45.4% semispan (fig.2) where clean wing tests had demonstrated that there was little variation in spanwise pressure distribution and hence the flow approximated to sheared wing conditions. It was agreed that the unrepresentative fuselage and the high wing installation would be of little significance at this spanwise station.

The nacelle profile was based on an early Rolls-Royce design for the RB.207 engine and this was matched to the local wing chord to obtain in effect a 1/20 scale model of a typical installation (fig.3). A NACA 1.85.45 external profile[1] was chosen for the forward fan cowl since on an isolated nacelle this would ensure a small spillage drag down to a relatively low mass flow, and a drag-rise Mach number at low incidences beyond the range of the current tests. The fan cowl contraction ratio is 1.25 and the profile from the highlight to the throat approximates to an ellipse. The boat-tail angle of the fan cowl is 13.5°. Compared with the original Rolls-Royce nacelle, the gas generator cowl has an enlarged exhaust nozzle to obtain a mass-flow ratio of about 0.7 at the inlet of the free flow nacelle whilst retaining dimensions of the correct order for the fan cowl nozzle. The gas generator cowl had a boattail angle of 16.5°. Both the fan cowl and gas generator ducts had a small contraction at exits.

The nacelle centre-line was parallel to the local wing chord (this was $1^{\circ}20'$ nose down, relative to the HS.681 wing and fuselage datum), and the nacelle was axisymmetric The positioning of the nacelle relative to the local wing section is shown in fig.4. A large nacelle under a low wing would require to be positioned vertically as close to the wing as possible and hence, the vertical distance from the wing was selected such that the wing boundary layer and fan cowl wake would not quite merge. In practice the fan cowl would require to be ahead of the wing in order to operate thrust reversers (unless of course the cowl were lengthened rearwards to incorporate exhaust nozzle silencers) and the positioning of the fan cowl ahead of the wing is typical of the spacing required.

The pylon design is defined in fig.4. A NACA 0012 profile was chosen for the original pylon section adjacent to the wing (fig.4A) in order (a) to have a well rounded leading edge, since on an aircraft the sidewash would vary considerably under different flight conditions, (b) to have the peak suction on the pylon well forward in order not to coincide with the peak suction in the wing lower surface distribution (fig.10) and (c) because a 12% thick pylon was

the minimum that could be used to duct sufficient air for the blown nacelle configuration to be described shortly. Aerodynamically, an R.A.E. 100 12% section would probably have been a better choice as the included angle at the trailing edge of the NACA 0012 aerofoil is 16° as compared with 11.8° for the R.A.E. 100 section. However the latter section would not have been so suitable for matching with the existing air duct position in the HS.681 model wing.

The pylon extended from 5% chord to 70% chord at the wing in order to have the leading edge well aft of the wing stagnation region, and the trailing edge at a typical rear bulkhead position. The pylon leading edge was defined by a line from the wing to the crest of the fan cowl and the trailing edge by a line from the wing to the gas generator exhaust nozzle. At the fan cowl the pylon forward section was changed to have a 10% R.A.E. 101 profile, to reduce the possibility of a suction peak in the vicinity of the cowl crest and a consequent local reduction in drag-rise Mach number. By not taking the leading edge forward of the crest this possibility was further reduced. The sections between the NACA 0012 profile and the R.A.E.101 profile were faired linearly.

The chord of the pylon increases rapidly with distance from the wing and it was decided that the pylon should have a constant maximum thickness. To achieve this the NACA 0012 shape was retained for the rear of the pylon and the length of the R.A.E.101 forward section at the fan cowl was determined from the maximum thickness. As a consequence a triangular area was obtained of constant maximum pylon thickness. This was beneficial in that the pylon thickness was constant in the region of the fan nozzle which simplified the design inside the nozzle, and also in making the design of the pylon compressed air ducting easier.

A pylon camber was chosen, defined by the model clean wing pressure distribution for a local $C_L = 0.48$ at $M = 0.71$. This is compared with a camber line for a local $C_L = 0.34$ at $M = 0.71$ in fig.5. The high rate of camber that would be required adjacent to the leading edge was ignored, since it was difficult to define this from the experimental data, and in any case incorporation of the extreme flow angles adjacent to the stagnation line would be impractical. In addition, the manner in which the flow deviations were propagated forward and below the wing was unknown and this would significantly affect the camber of the highly swept pylon leading edge. Consequently the camber was modified at the leading edge as indicated by the chain dotted lines. The camber at the relatively high C_L was chosen, since this aided model design by limiting variations in camber to aft of the maximum thickness station, thus reducing vertical distortions in the region in which the compressed air pipes were ducted through the pylon, and also by

avoiding variations in the camber of the pylon at the fan cowl nozzle. It was also hoped that the small change in camber due to choice of the higher C_L conditions would not have too much effect on the flow. Also, it should be remembered that in practice, the presence of the nacelle itself would modify the direction of the flow streamlines over the wing. The camber was reduced linearly to zero on a section at the maximum pylon span (i.e., at the gas generator nozzle), along lines of constant pylon thickness. The propagation parallel to the pylon trailing edge rather than say vertically downward, was considered to be not unreasonable in the vicinity of the nacelle.

A preliminary model test to check that the fundamental wing-nacelle geometry was satisfactory, indicated that at the pylon leading edge the curvature of the pylon surface approaching the maximum pylon thickness was too high for the local flow conditions (this will be discussed in detail in section 4). Consequently the pylon leading edge was extended forward locally adjacent to the wing, to mate with the wing at 2% chord (which was still aft of the stagnation point for normal operating conditions), and to have a leading edge sweep angle of $79^{\circ}16'$. The pylon leading edge sweep adjacent to the nacelle remained unaltered at $84^{\circ}58'$. The upper forward section of the pylon was then revised to have a NACA 0010 profile and the forward profile of the lower section was faired smoothly into this, resulting in a lower section of increased length and the same thickness form. In effect this provided the lower pylon with a NACA 00046 forward section. As discussed later in section 4, the local flow at the pylon leading edge was found to be satisfactory after this modification, and hence this design was used for the general test series.

Four different configurations were then tested. A fully pressure plotted version of the above nacelle/pylon installation, a nacelle supported by a minimum pylon to determine the effects on the wing of the nacelle alone, a fully pressure plotted nacelle with a shrouded gas generator to simulate the fan jet flow, and a nacelle with a blown fan jet operating at representative pressure ratios.

The pressure points on the fully pressure plotted nacelle are indicated in fig.3. Both sides of the nacelle and pylon were identically pressure plotted. In addition, the wing upper and lower surfaces were pressure plotted along the chord lines shown in fig.2. Besides the external pressures, static pressures were also measured internally at the fan and gas generator nozzles on the nacelle in order to assess the internal drag of the nacelle for force data reduction.*

---

* Drag data is not included herein as the internal drag is still being determined. Calculation of the internal losses has been complicated by the use of curved surfaces (the inner wall of the fan cowl for example). In similar model installations it is recommended that ducts having straight walls should be used wherever possible.

Overall forces on the model were measured for the fully pressure plotted and minimum pylon installations only. For the blown nacelle, the balance constraints due to the compressed air ducting could not be assessed and the particular shroud installation tested was not suitable for force corrections. The "minimum-pylon" installation is drawn in fig.7. The pylon was of constant chord NACA 0010 section. At the wing the pylon extended from 10% chord to 27% chord, to avoid the need for pylon camber. It was not possible to obtain pressure measurements on the nacelle and pylon, but wing pressures were measured.

The shrouded nacelle is shown in fig.8. Unreported tests on a different model at A.R.A. had suggested that the fan jet boundary would be sensibly of the same outside diameter as the fan nozzle at the plane of the gas generator nozzle. Hence a simple parallel cylinder shroud was designed for the fully pressure plotted nacelle, on the basis that if this were successful, then drag corrections for a pressure cylinder would be relatively simple. To try and obtain the same intake flow as with the previous models, the fan nozzle area was not altered, and the thickness of the shroud was absorbed by a slight expansion of the "jet" boundary at the nozzle exit.

The blown nacelle design is shown in fig.9. A total pressure of 1.5 atmos. was required at both the fan nozzle and the gas generator nozzle in order to obtain representative exhaust pressure ratios. To duct the required fan nozzle mass flow alone through the pylon, 300 p.s.i. was required, and 500 p.s.i. was needed in order to pipe this air through an existing duct in the wing. The only suitable air supply at A.R.A. was an intermittent 4000 p.s.i. system primarily used to drive the hypersonic tunnel facility. Since running times would only be of several minutes duration with this supply, and the gas generator exhaust flow was not likely to have any significant interference effects[2], it was decided that only the fan nozzle would in fact be blown. It was also considered desirable that the intake should not be faired in, because the fairing would be extremely large so that the resultant flow distortion could well mask any jet effects. Hence it was decided to have free flow through the gas generator nacelle and to attempt to obtain the basic free-flow nacelle pressure distribution on the fan cowl forebody by the choice of a suitable intake bullet. The bullet was designed by extrapolating data in ref.3, on the assumption that similar pressure distributions would be obtained on a particular NACA cowl with and without a spinner present, provided that the predicted critical Mach numbers were identical. In order to choose a bullet which satisfied this condition and which would not have a serious separation at the inlet, particularly at incidence, the throat diameter of the fan cowl had to be increased, so that the cowl contraction ratio was reduced to 1.072. The internal lip shape was made a constant radius and from experimental data at A.R.A. it was not expected that this would significantly affect the external cowl lip pressure distribution at the test Mach numbers. The throat area was matched to the exhaust

nozzle area to obtain an intake flow which simulated a mass flow ratio slightly in excess of 0.7 in order to reduce the possibility of separated flow from the fan cowl lip should the bullet design be unsatisfactory. The bullet finally chosen was a NACA 1.70.60 i.e., a NACA I profile and a diameter and length of 0.7 x and 0.6 x maximum fan cowl diameter respectively. Because of the space required inside the fan cowl for the compressed air ducting, the free stream intake flow was required to turn rapidly inwards aft of the intake throat. The area distribution was carefully controlled to reduce the possibility of flow separation in this duct.

A satisfactory exhaust flow distribution was obtained by the use of the two perforated plates indicated in fig.9. A mock-up of the compressed air system from the pylon inlet to fan nozzle exit was used to develop this system. With no control on the exit flow, the circumferential distribution was poor, with the majority of the air flowing out of the bottom of the nozzle, whilst radially, a typical pipe flow distribution was obtained, with the flow falling off rapidly at the sides of the annulus. Control of the distribution was obtained using a symmetric hole array in the perforated plate nearest the nozzle, whilst varying the open hole distribution of what was otherwise an identical array, on the inner plate. This achieved a reasonably uniform distribution around the circumference and a square distribution across the width of the nozzle.

3. TEST CONDITIONS

The model was tested at $0.6 \leq M \leq 0.81$. The tests were not taken to a higher Mach number, because it was considered that the clean wing characteristics would then be unsatisfactory.

At these Mach numbers the Reynolds numbers were as follows:

M	R_C	R_D
0.6	3.6×10^6	1.6×10^6
0.81	4.3×10^6	2.0×10^6

where R_C is based on the local wing chord at the nacelle position and
R_D is based on the fan cowl maximum diameter.

Transition was fixed on the wing with a 0.15 inch wide roughness band at 0.05 chord using ballotini of 0.0049 - 0.0059 inch diameter and Araldite adhesive.

On the fan cowl a band of 0.0030 - 0.0035 inch ballotini was situated 0.3 to 0.6 inches aft of the highlight, and the same size ballotini was also used on the bullet 0.3 to 0.6 inches aft of the apex.

On the inboard side of the pylon the roughness band was between 0.2 to 0.6 inches from the leading edge measured along the normal from the leading edge, whilst on the outboard side the band was 0.25 to 0.40 inches from the leading edge when viewed from the front. The ballotini used was again 0.0030 - 0.0035 inches diameter.

The transition fixing was checked using acenapthene.

4. DISCUSSION OF TESTS

As previously noted, a free flow model with the original pylon as in Fig.4A was tested first. Force data indicated that the installation had an interference drag that was not unacceptably high. However oil flow runs at $M = 0.71$ at $\alpha_b = 3^o$ and 5^o showed that there was an undesirable separation on the outboard side of the pylon at the leading edge, plate 1A. Due to the cross flow, the flow at the pylon leading edge was virtually parallel to the wing leading edge adjacent to the pylon wing junction. The section normal to the pylon leading edge was then found to be excessively flat with an extremely high rate of change of curvature near the maximum thickness (Fig.6); this evidently causes the flow separation. Hence the leading edge was revised as described in section 3. The pylon profile normal to the leading edge, although bluff was now of a reasonable shape and repeat tests at the earlier oil flow test conditions, demonstrated that the separation was no longer present (Plate 1B). Due to the cross flow the stagnation line was on the inboard side of the pylon leading edge, Plate 2, and moved aft as incidence was increased. A region of separated flow at the rear of the fan cowl and inboard of the pylon was induced by the cross flow at moderate incidences, Plate 3, and it will be observed that the appearance of this separation is related to the position of the stagnation line.

The flow separated at the trailing edge on both sides of the pylon, Plate 4. This was probably due to the large trailing edge angle of the NACA 0012 basic pylon section. The pylon wake at the wing surface suggests that the pylon should have been more cambered at the rear, but the oil flow in the wing boundary layer adjacent to this may not be in the true local external flow direction.

The oil flow tests with the minimum pylon demonstrated that the forward influence of the wing in itself was sufficient to cause flow separation on the rear upper surface of the fan cowl, Plate 5. Comparison of wing pressure distributions for the minimum pylon with those for the free flow nacelle and for the clean wing, Fig.10 is useful in demonstrating

the effect on the wing flow of both the nacelle and the pylon. (The minimum strut data is for the lower surface only). The first point to note is that there is an increase in suction on the forward lower surface, and a decrease at the rear when the nacelle is present, so that in effect the peak suction on the lower surface is moved forward. The shape of the revised pressure distribution is little affected by the presence of the pylon. In fact the only significant change with the pylon present is to increase the peak suction level on the inner wing. Hence one concludes that in the absence of jet effects at least, the pylon shaping should be aimed at minimising the interference on the wing, inboard of the pylon. The results from the blown nacelle tests, to be discussed later, indicate that this conclusion is still applicable. On the lower surface the presence of the nacelle in itself has not increased the peak suction value above that of the basic wing except that at very low incidence. In fact on the outer wing panel the value is reduced. However with the pylon present the maximum surface velocities on the inner panel are greater than those on the clean wing. There is apparently little change in the pressure distribution on the upper surface of the inner wing in the presence of the nacelle and pylon, although additional pressure points would be useful adjacent to the leading edge in order to confirm this. On the outer wing there is a significant reduction in the peak suction and this is probably the reason for the reduction in the separation that occurs over the front of the wing at the highest incidence. At the test conditions, there is no noticable effect on the trailing edge pressures due to the presence of the nacelle and pylon.

Now let us consider the blown fan nozzle tests. It was first necessary to confirm that the blown configuration was consistent with the free flow models, before attempting to determine the effect of blowing at a representative pressure ratio. Hence the blown nacelle was tested with the fan nozzle running both at $H_J = H_o$ and at $H_J = 1.5\ H_o$. Typical pressure distributions are shown for the wing stations in Fig.11 and at the wing-pylon junction in Fig.12. These figures demonstrate that in general the data from the blown nacelle at $H_J = H_o$ are sensibly identical to that from the free flow nacelle. At a jet pressure ratio $\frac{H_J}{H_o} = 1.5$ the shape of the pressure distribution is unaltered, but the peak suction level is increased compared with the results from the free flow nacelle. This effect is reduced with increase in incidence, Fig.11, and from the inboard distributions, Fig.12, there is also a suggestion of a Mach-number freeze on the wing surface pressures, beyond which the suction level does not rise. Thus jet effects may be less significant at free stream Mach numbers above those of the present tests. At the wing/pylon junction the

increased suction with blow occurs at about 25% actual wing chord or 43% pylon chord on both sides of the pylon. At M = 0.77 this is the source of a relatively unswept strong shock wave on the inner wing, Plate 8. At M = 0.79, Fig.12, the peak suction on the outer wing is rapidly approaching the suction level of that on the inner wing, and hence a fairly strong shock wave might be expected here too at slightly higher Mach numbers. Although the suction increase is aft of the maximum thickness line on the pylon it is ahead of the crest on the wing, so that the presence of the shock wave on the lower surface is not as damaging as might at first appear. On the wing the additional suction on the lower surface would result in a local loss in C_L, although at the higher Mach number conditions where the suction peak is of the same order, jet on or off, then there is a slight rise in pressure level over the rear panels and hence possibly, a slight increase in C_L at a given incidence.

Variation of the gas generator pressures with incidence at M = 0.71, and with Mach number at $\alpha_b = 3\frac{1}{2}^o$ is given in Figs.13 and 14. The surface pressures at $H_J = H_o$ are basically the same as those for the free flow nacelle. With the fan jet exhausting at 1.5 H_o there is a suction increase which reaches a maximum at about 75% of the gas generator cowl length.

At this pressure ratio, it is estimated that the fan cowl exhaust is subsonic to about M = 0.71 (an assessment of the internal duct flow for the free flow nacelle indicated that the exit C_p was positive). Even at M = 0.77 when the nozzle is definitely choked, the pressure ratio is evidently too low for strong shocks to form in the exhaust flow, except where imposed by the wing-pylon-nacelle interference. In assessing the local Mach numbers on the gas generator cowl it should be remembered that the relevant total pressure is of the order of 1.5 H_o. For example a shock is present at M = 0.71 at the suction peak on the inboard side of the pylon. This causes a flow separation locally at the rear of the gas generator at the lower incidences. As might be expected the gas generator suction peak is adjacent to that at the wing/pylon junction, Fig.15. Plate 7B shows the oil flow on the outboard side of the pylon and nacelle when blowing at $H_J/H_o = 1.5$ at M = 0.71 with $\alpha_b = 5.1^o$. There is a thick layer of oil present on the gas generator cowl. This is due to oil which has collected inside the "base" of the fan nozzle as the tunnel is brought up to speed flowing out once blowing begins. However instead of being scrubbed away the oil then stagnated. It has been suggested that this is because of the low temperature of the gas generator surface caused by throttling of the internal air. The uneven distribution of the oil on the gas generator cowl is probably associated with local cooling variations, through the expansion of the air at the pylon duct outlets. (Note that the dark band

on the fan cowl, and the similar band at the rear of the gas generator cowl are pressure tube runs, not air flow induced effects).

Plate 7A shows the flow on the upper side of the fan cowl at M = 0.71 at $\alpha_b = 5.1^o$ with $H_J/H_o = 1.5$. Unlike the free flow nacelle at this condition, Plate 3B, there is little sign of a separation inboard of the pylon at the rear of the fan cowl. However this is not necessarily a jet effect since no separation bubble was observed prior to blowing. The fan cowl pressure distributions, Fig.16, show that the intake was effectively operating at a higher mass flow ratio (i.e. at reduced lip suction values) with $H_J = 1.5\ H_o$ and hence the boundary layer at the rear of the cowl may have been modified. To judge from the lip suction the intake was operating at an effective mass flow ratio of about 0.66, as against a free flow nacelle mass flow ratio of about 0.60, as suggested both by the lip pressures and by internal pressure measurements. The blown nacelle was of course designed to run at a slightly higher mass flow ratio than required, to avoid the possibility of lip separations if the bullet design were not successful. On the other hand the free flow nacelle was intended to operate at a mass flow ratio of order 0.7, but the flow was less than this due to there being positive base pressures at both nozzle exits. Another point to note is that the blown nacelle inlet flow was satisfactory despite the presence of the expected flow separation at the spinner crest, Plate 7A.

Yawmeter tests with the clean wing had indicated that in pitch, the flow in the region of the fan cowl intake was closely parallel to the free-stream and that the sidewash was about 3^o. It is therefore consistent to find that the separation bubble which forms at the lips was longer on the upper outboard side, Plates 3B and 5. The oil flow photographs were obtained wind-off after running at the specified condition for several minutes, followed by a rapid tunnel shut down. The latter accounts for the oil under the separation bubble apparently having run back along the cowl in the photographs. Fan cowl distributions, Fig.16, are consistent with the oil flow, in that under low spillage conditions with no significant separations present, the maximum peak suction at the lip occurs where the relative incidence at the lip is highest, i.e., intermediate to the top and side outboard pressure distributions. Incidentally, the top inboard and outboard pressure distributions are from a single row of pressure holes ahead of the pylon, which then divides to pass each side of the pylon. The pressure rise at about 40% cowl length at the top is due to the pressure field ahead of the pylon.

Finally we come to the shrouded gas generator tests. The lip pressures Fig.16, suggest that the intake flow is slightly greater than that with the

free flow nacelle, and hence intermediate to that of the free flow and blown nacelles. Despite this, Plate 6 shows that a significant separation occurs inboard of the pylon at the rear of the fan cowl at M = 0.71 even at 2.9° incidence. In addition Fig.16 shows that there is a general pressure rise all over the fan cowl, due to the presence of the shroud. Hence one concludes that the pressure rise at the rear of the fan cowl due to the presence of the shroud does not simulate the presence of the exhaust jet. Even more important Fig.17 shows that the pressures at the lower surface of the wing, in the presence of the shroud, are akin to those of the clean wing in form at M = 0.71, and Fig.12 confirms that the peak underwing suction occurs further aft under different Mach number conditions with the shroud present. The magnitude of the peak suction is increased compared with the clean wing, and since this occurs in the vicinity of the crest of the wing the effect is significant. On the wing upper surface the peak suction at the lip was of greater magnitude than that for the blown nacelle configuration. Thus the results of the present tests with the shroud are not encouraging. However the parallel cylinder probably simulated too large a jet. Ref.2, for example, suggests that the jet boundary could contract over the rear of the gas generator cowl. In addition, the effect of the jet or shroud would be less if the nacelle were further from the wing in a vertical sense. Even so, it is obvious that one has to be very careful in using a shroud to simulate jet effects. The flow at the rear of the fan cowl could not be simulated (unless possibly if there were a gap between the shroud and the cowl, and there were not excessive outflow or inflow at the gap), and the shroud effects would require to be tested against a blown nacelle to ensure that the shroud was of satisfactory design. To be able to use a shroud would of course be very beneficial, where a continuous compressed air supply is not available, where sufficient compressed air cannot be passed through the pylon, and to simulate jet effects on a force model, assuming that the forces on the shroud could be determined satisfactorily. The shroud on this model was assembled around the basic free flow model, so that an internal throat was formed at the fan nozzle exit. There was then a relatively slow expansion until near the rear of the gas generator. This resulted in a supersonic flow being developed in this annulus, with an ultimate shock and separated flow from the gas generator. Consequently this particular configuration had a high drag. For a force model installation it would therefore be preferable to use an extended fan cowl nacelle, with no internal body.

REFERENCES

1. BAALS, DONALD D.
SMITH, NORMAN F.
WRIGHT, JOHN B.

The Development and Application of High-Critical-Speed Nose Inlets.

NACA Report 920, 1948.

2. RANEY, D.J.
KURN, A.G.

Interim Report on Wind Tunnel Measurements of Jet Interference for High Bypass Engines mounted on a Wing.

RAE Tech Memo Aero 975, March 1967.

3. NICHOLS, MARK R.
KEITH, ARVID L. Jr.

Investigation of a Systematic Group of NACA 1-Series Cowlings with and without Spinners.

NACA Report 950, 1949.

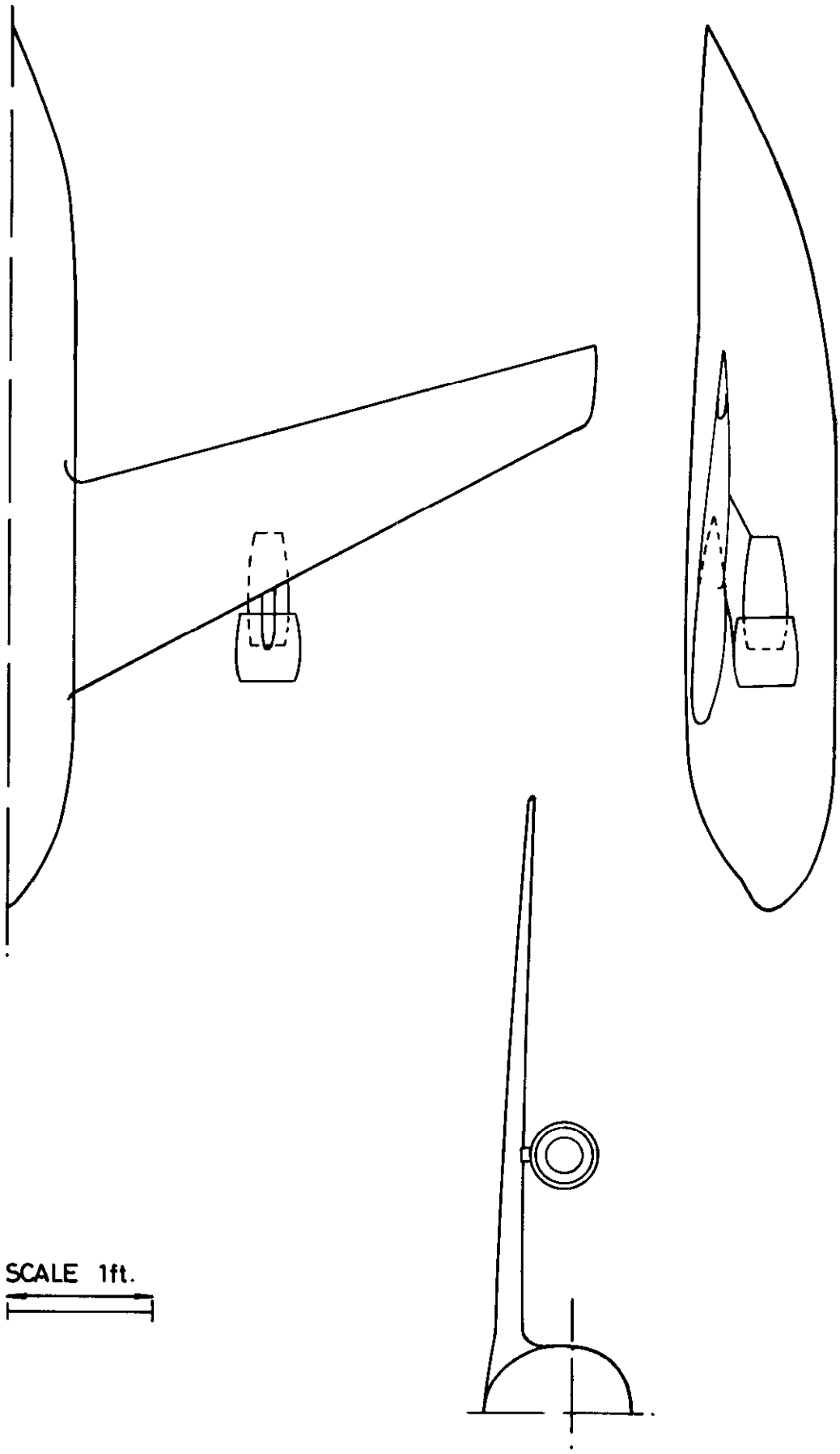

FIG. 1. GENERAL ASSEMBLY OF MODEL.

FIG. 2.

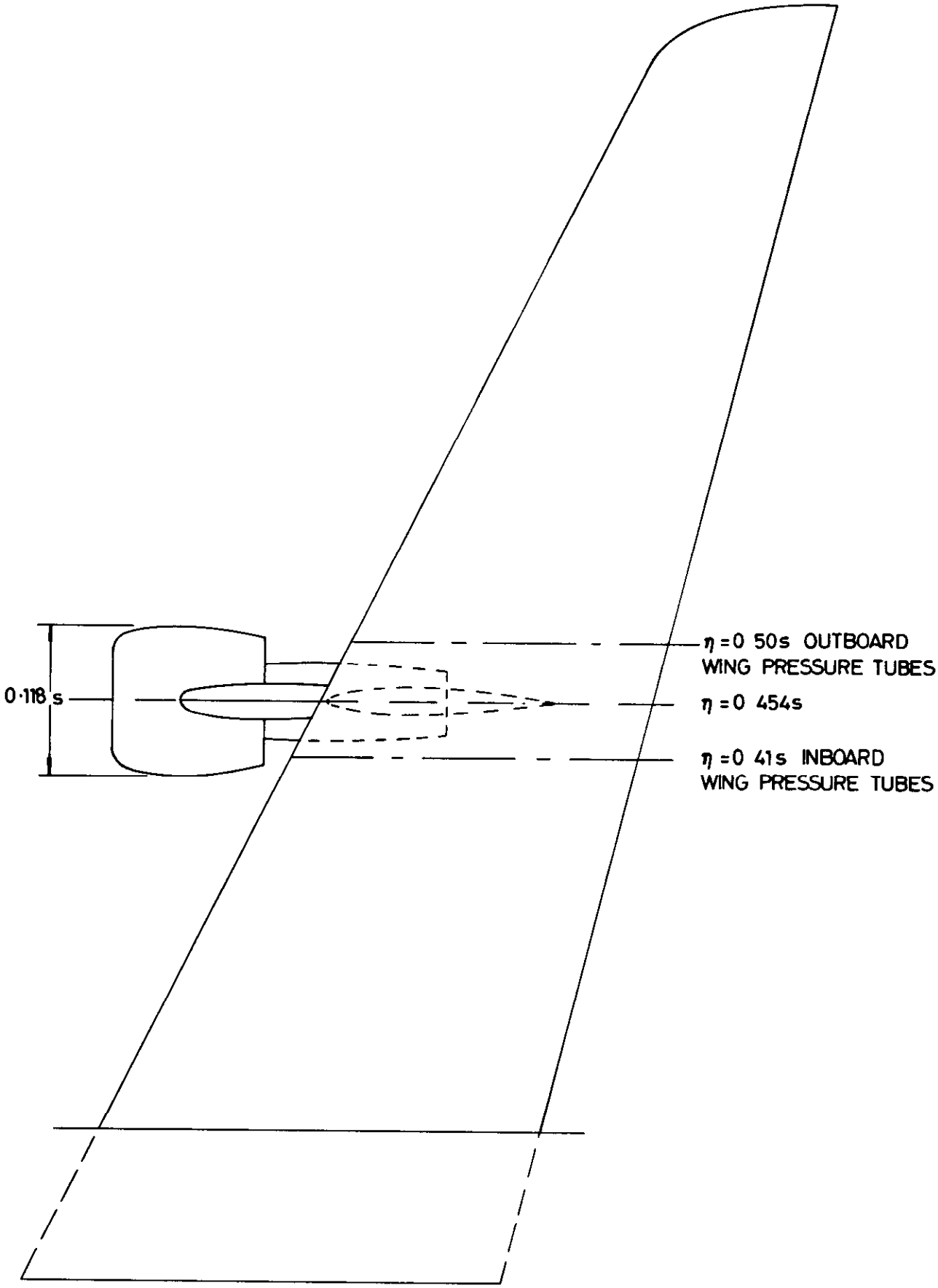

FIG. 2. SPANWISE NACELLE AND WING PRESSURE TUBE LOCATION.

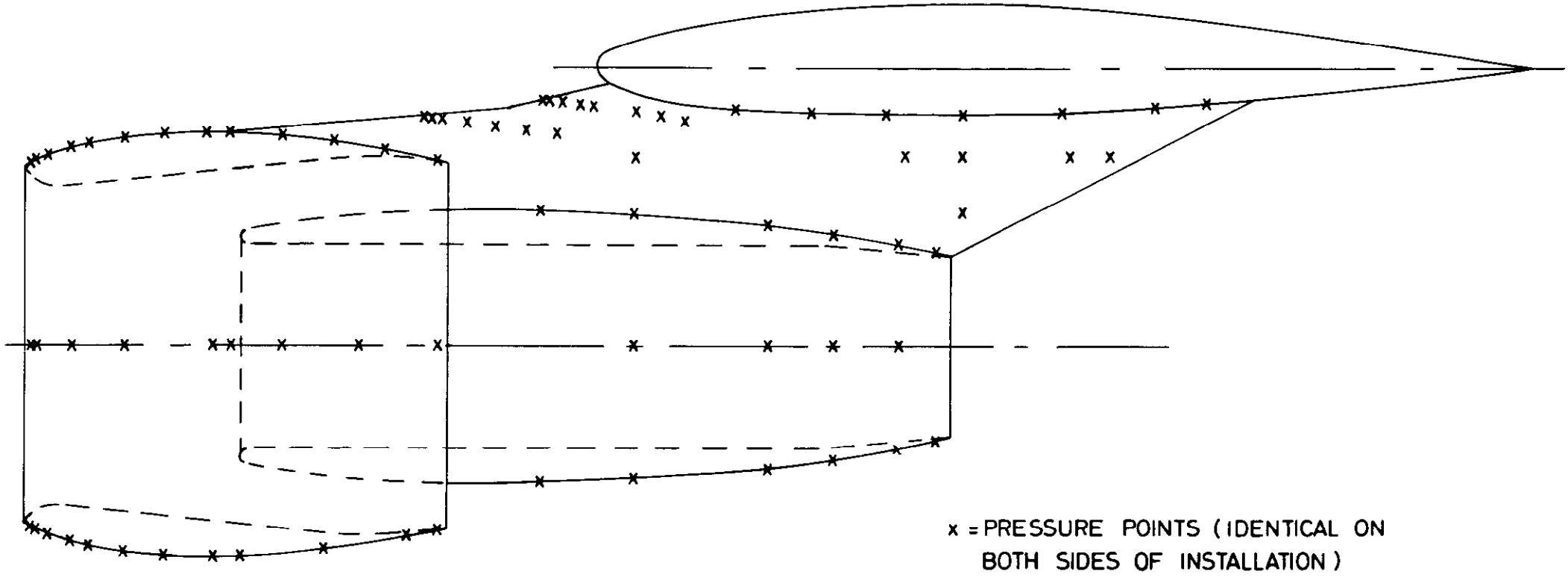

FIG. 3

FIG. 3. FULLY PRESSURE PLOTTED $\frac{1}{20}$ F.S NACELLE INSTALLATION.

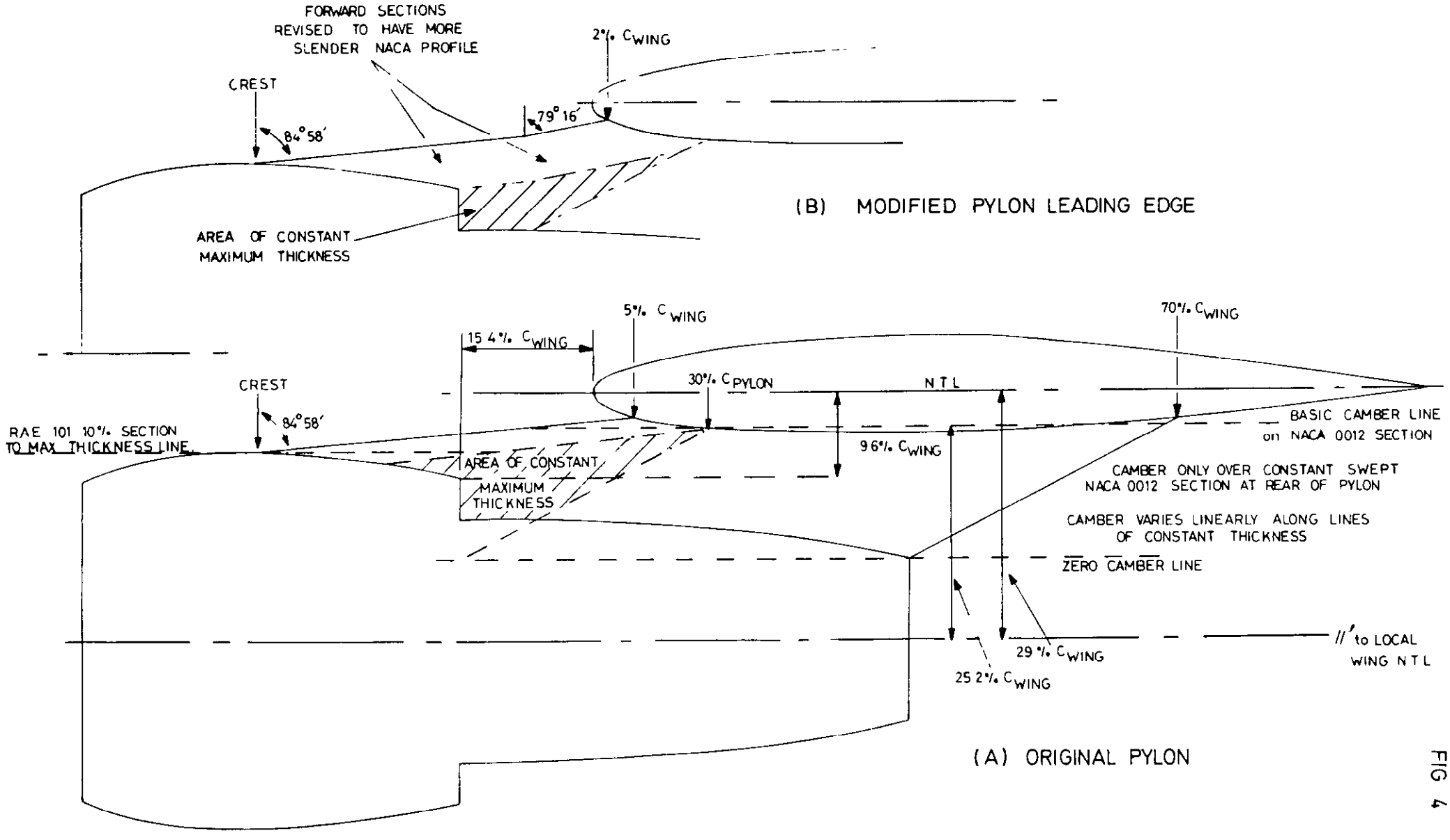

FIG 4

FIG4 NACELLE POSITION RELATIVE TO LOCAL WING SECTION AND (A) ORIGINAL PYLON, (B) MODIFIED PYLON

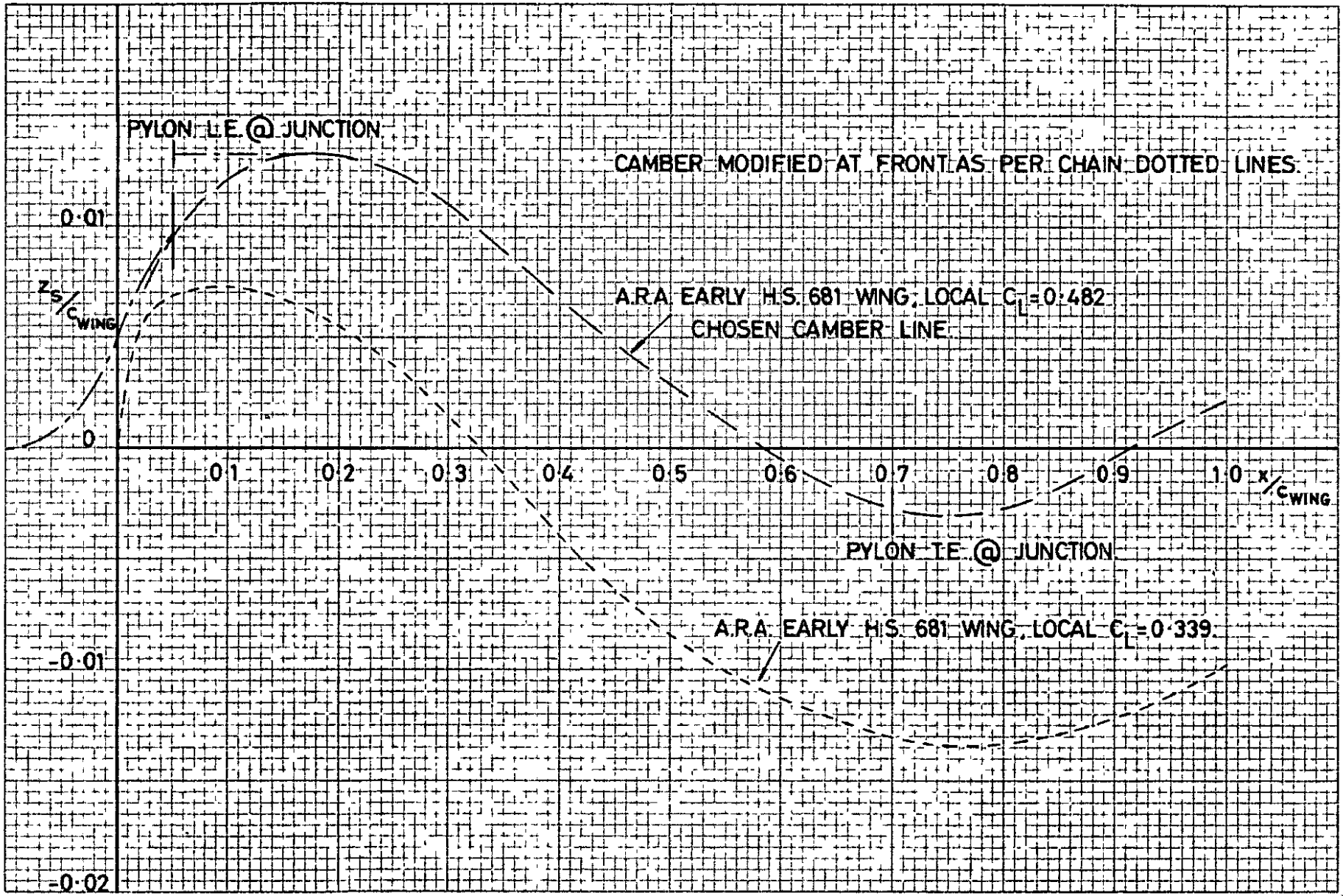

FIG. 5.

FIG. 5. COMPARISON OF CAMBERS FOR PYLON TO FOLLOW LOWER SURFACE STREAMLINES AT LOW AND MODERATE C_L AT $M = 0·71$.

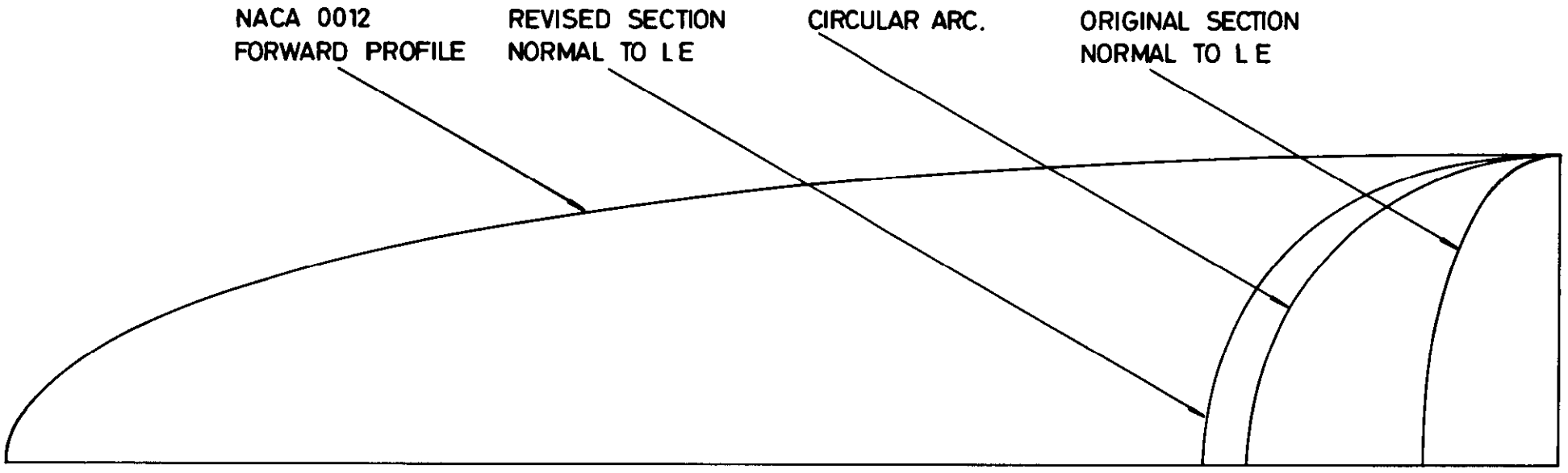

FIG. 6.

FIG. 6. WING ROOT PYLON SECTIONS. FORWARD OF MAXIMUM THICKNESS.

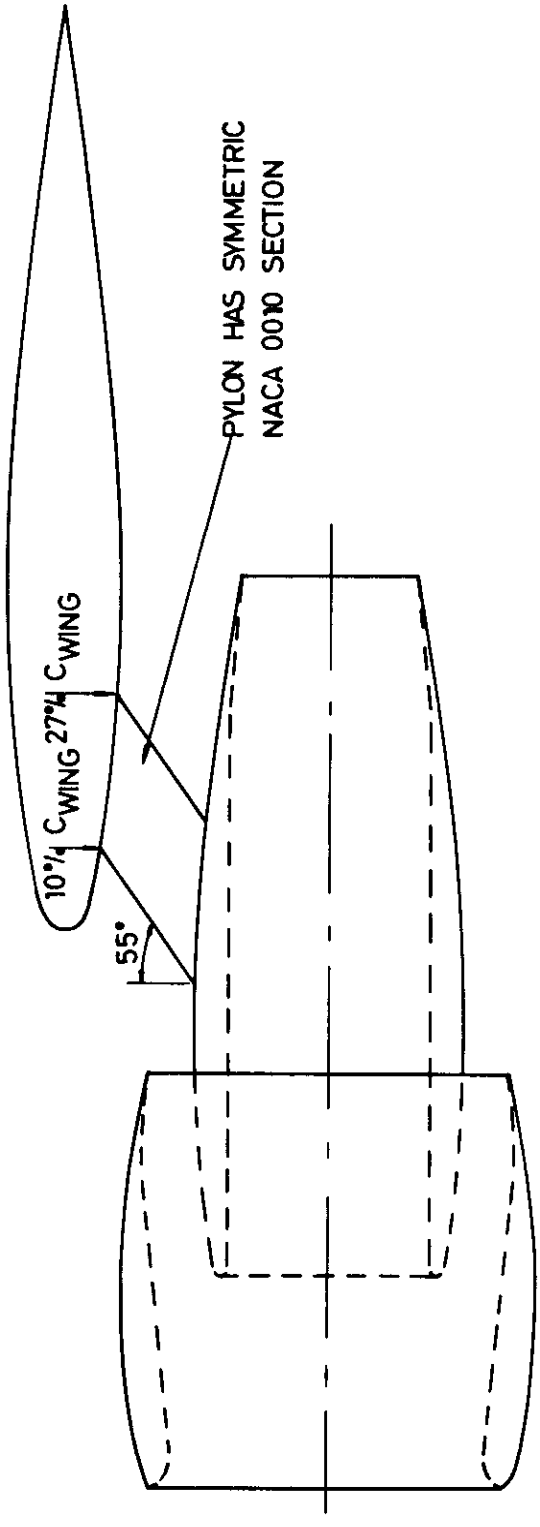

FIG. 7. MINIMUM PYLON INSTALLATION

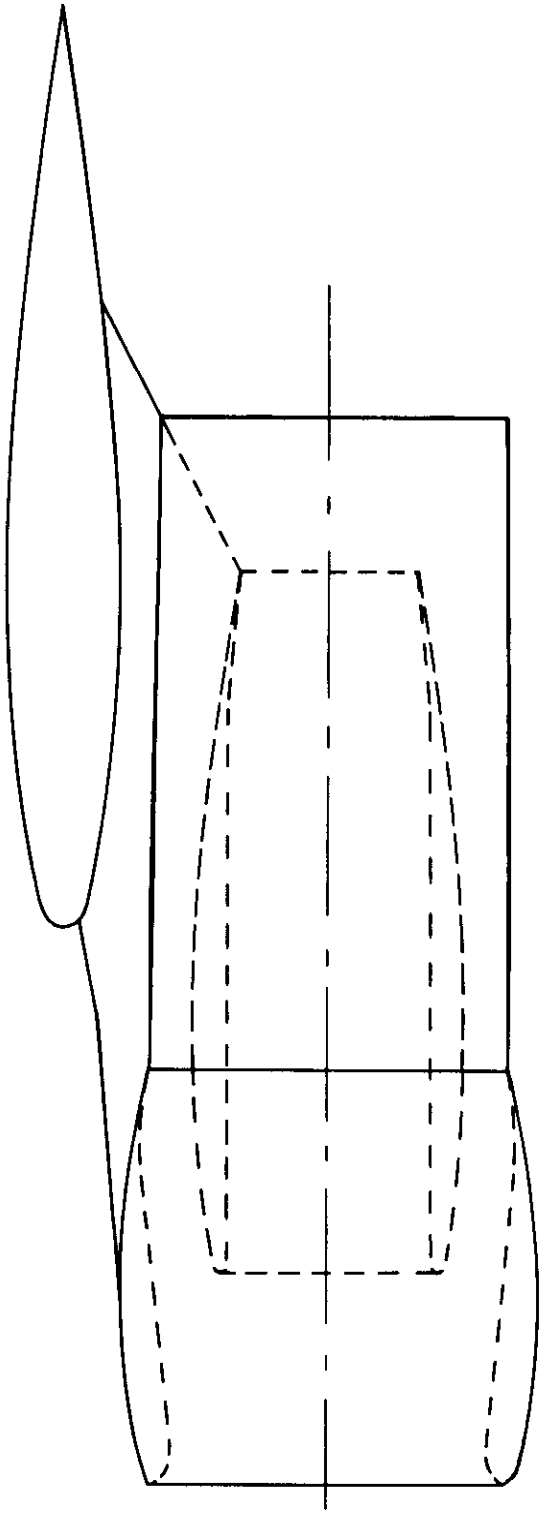

FIG 8 SHROUDED NACELLE INSTALLATION.

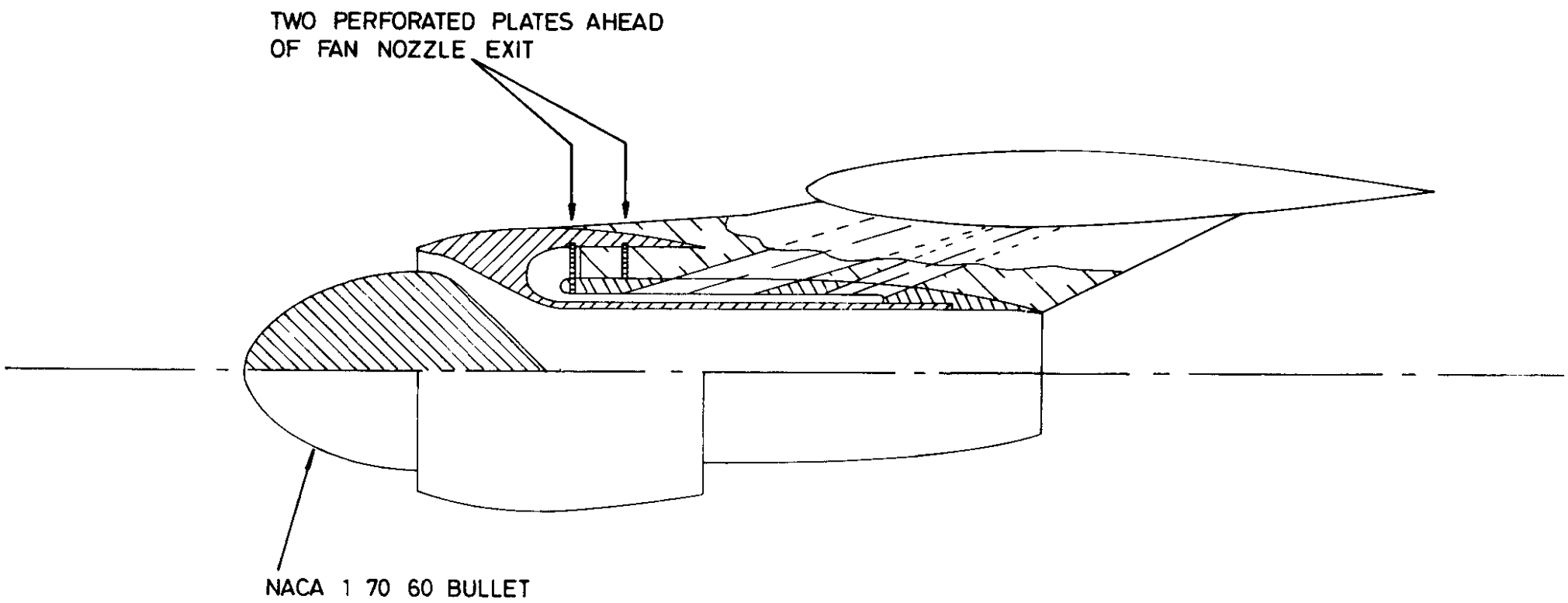

FIG. 9.

FIG. 9. BLOWN FAN COWL INSTALLATION.

FIG 10a

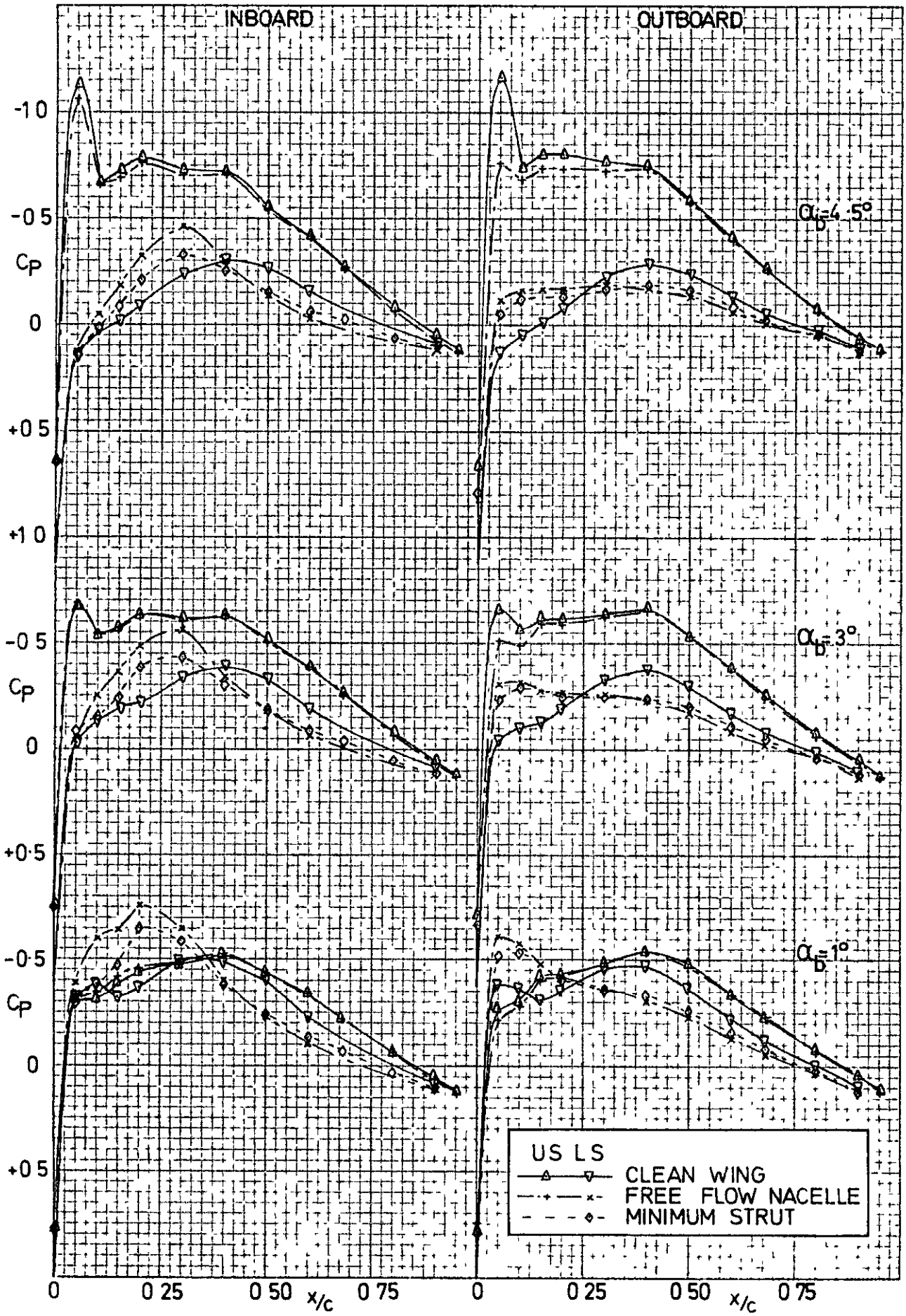

FIG 10a. EFFECT OF NACELLE AND PYLON ON WING PRESSURES AT M=0·71

FIG 10b

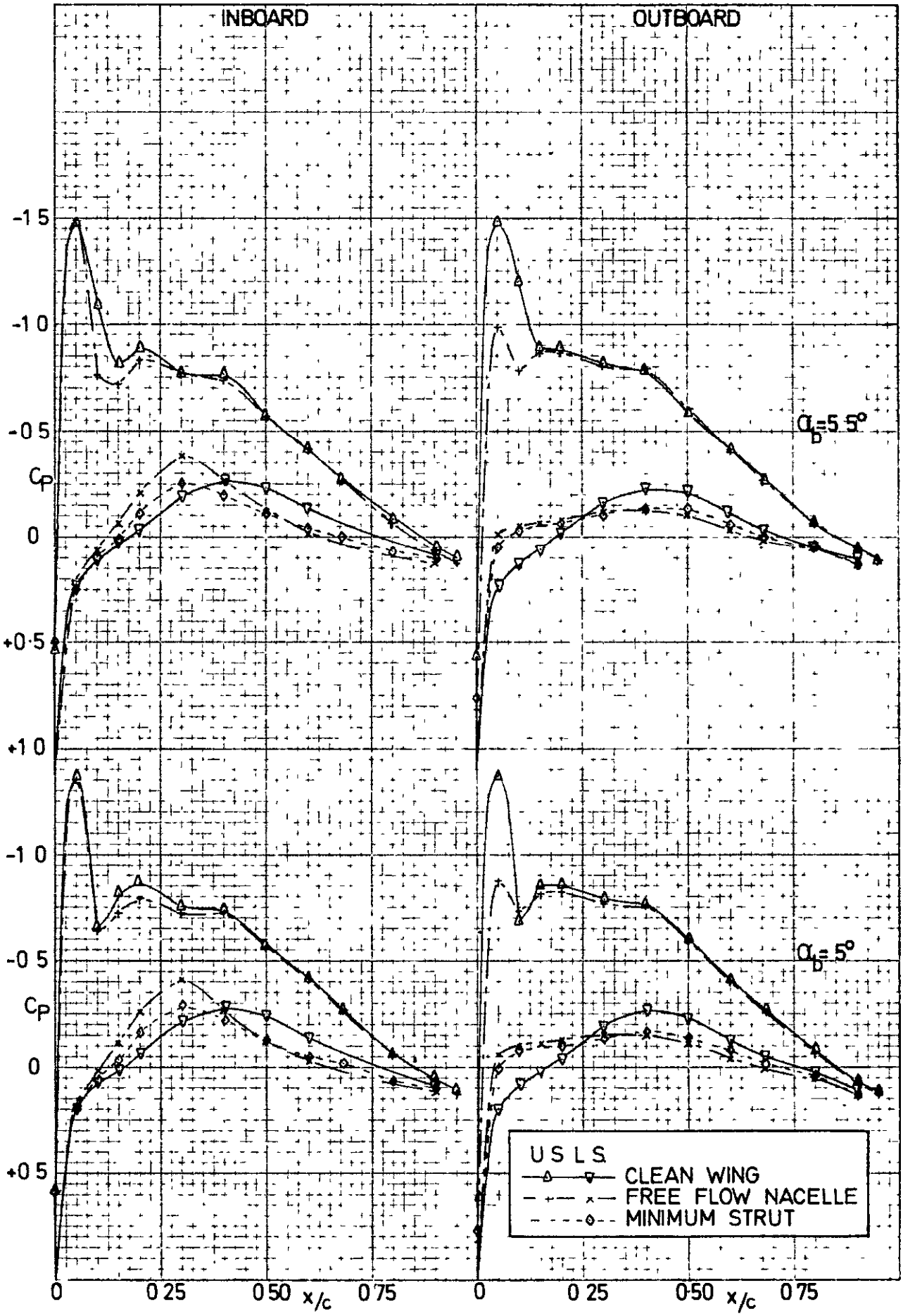

FIG 10 b. EFFECT OF NACELLE AND PYLON ON WING PRESSURES AT M=0·71

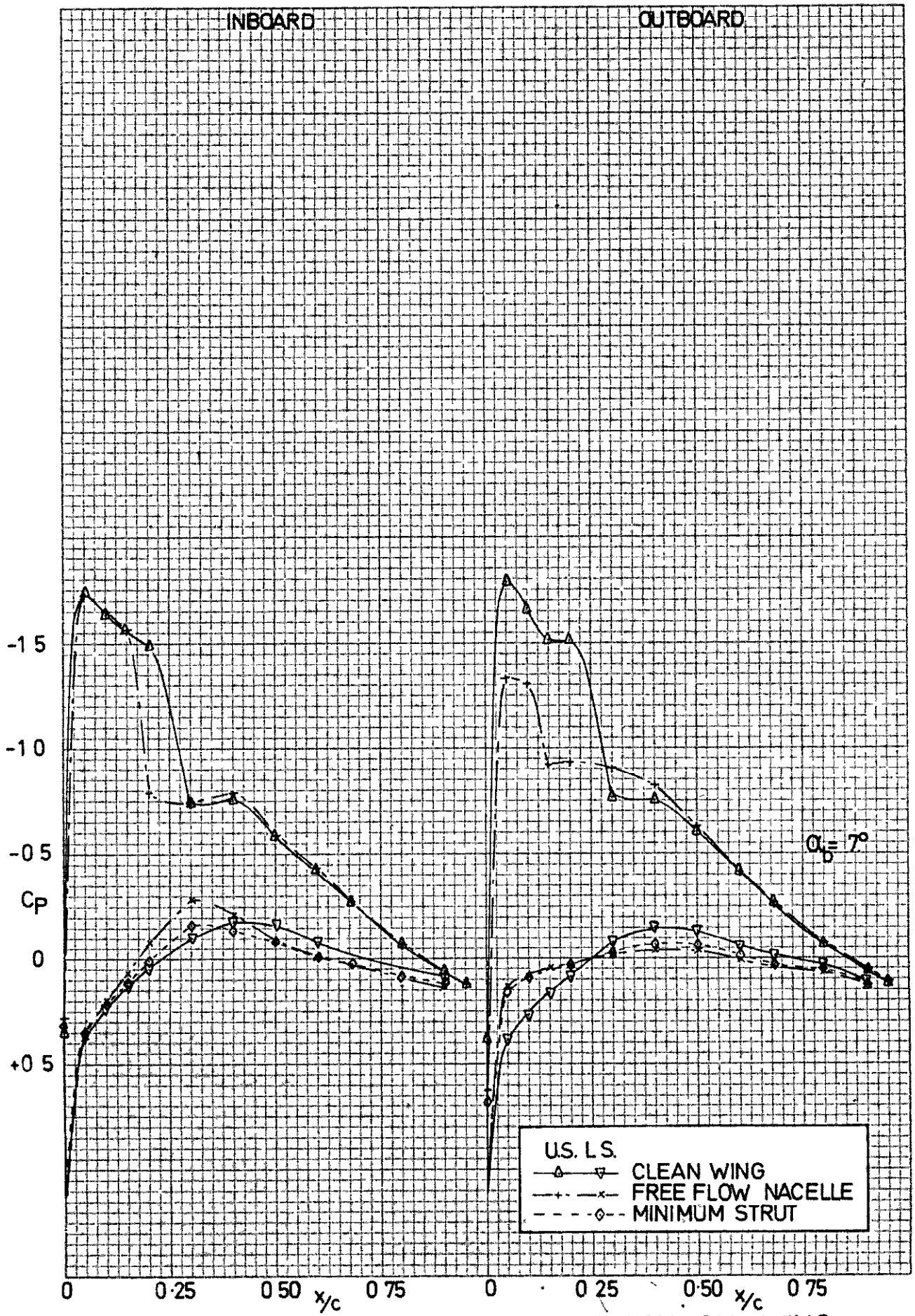

FIG 10c EFFECT OF NACELLE AND PYLON ON WING PRESSURES AT M=0·71

FIG 11

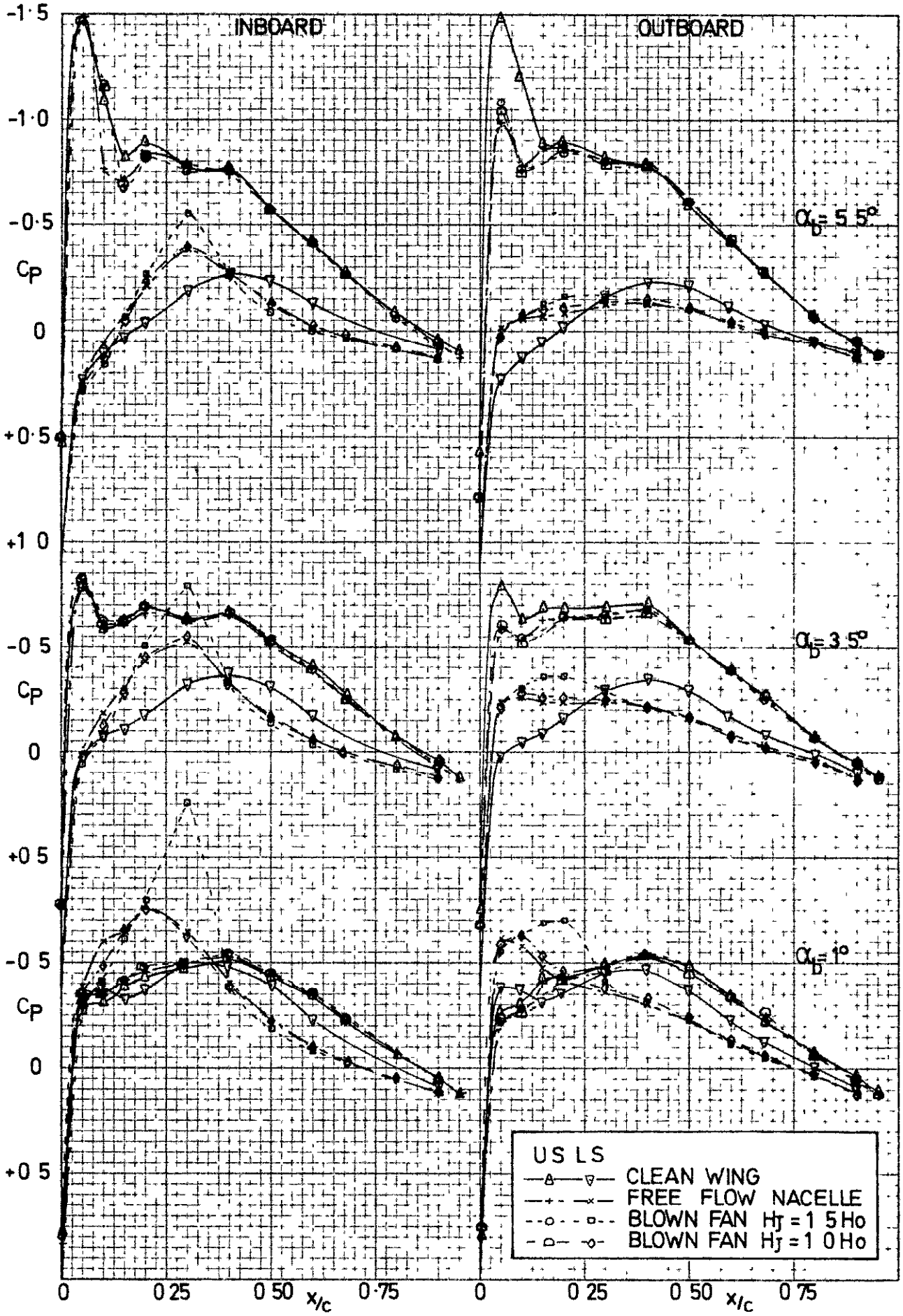

FIG 11. EFFECT OF FAN NOZZLE EXHAUST FLOW ON WING PRESSURES AT M=0·71

FIG 12a

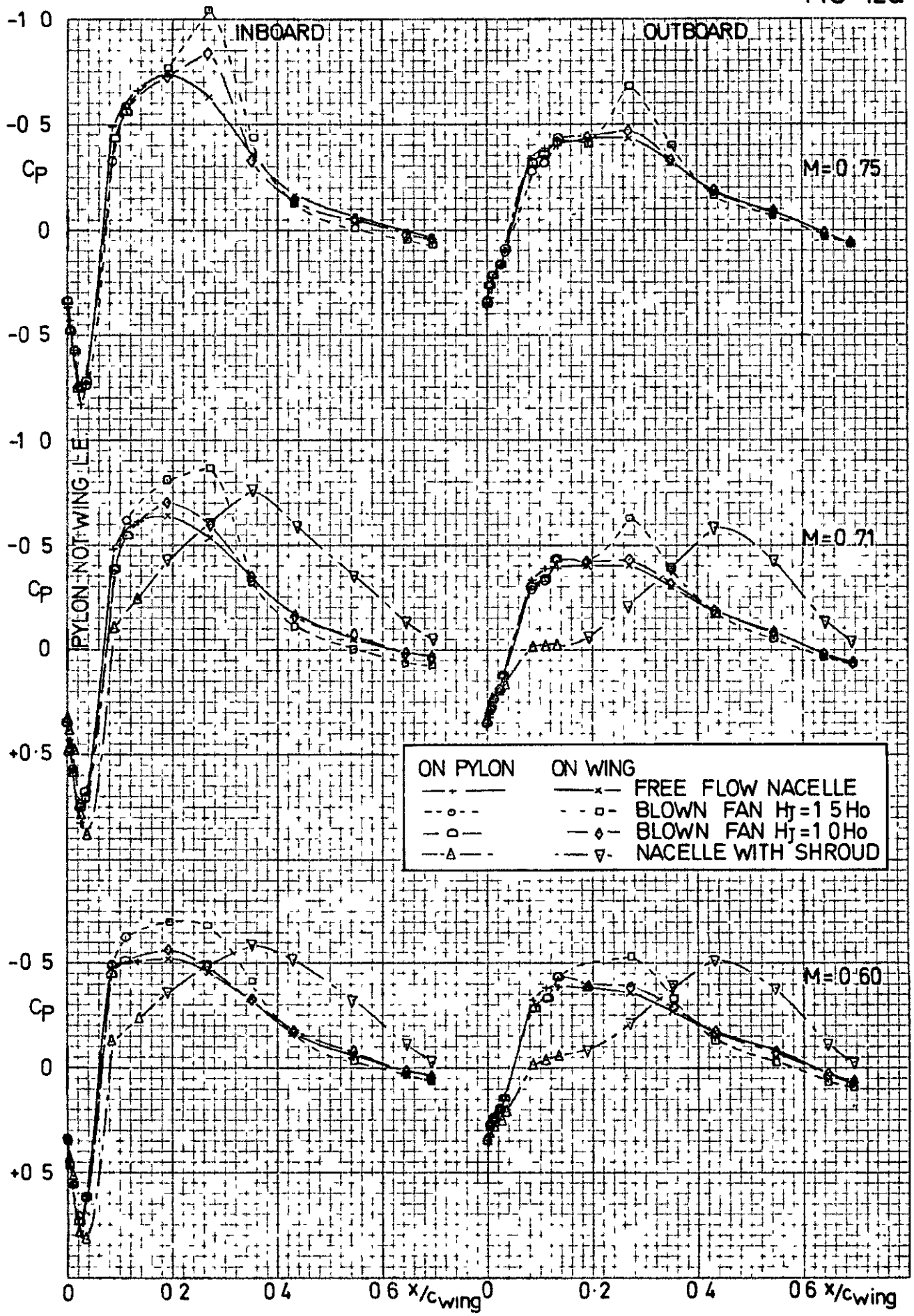

FIG 12a EFFECT OF FAN NOZZLE EXHAUST FLOW AND SHROUD ON PRESSURES AT THE PYLON - WING JUNCTION AT $\alpha_b = 3{\cdot}5°$

FIG 12b

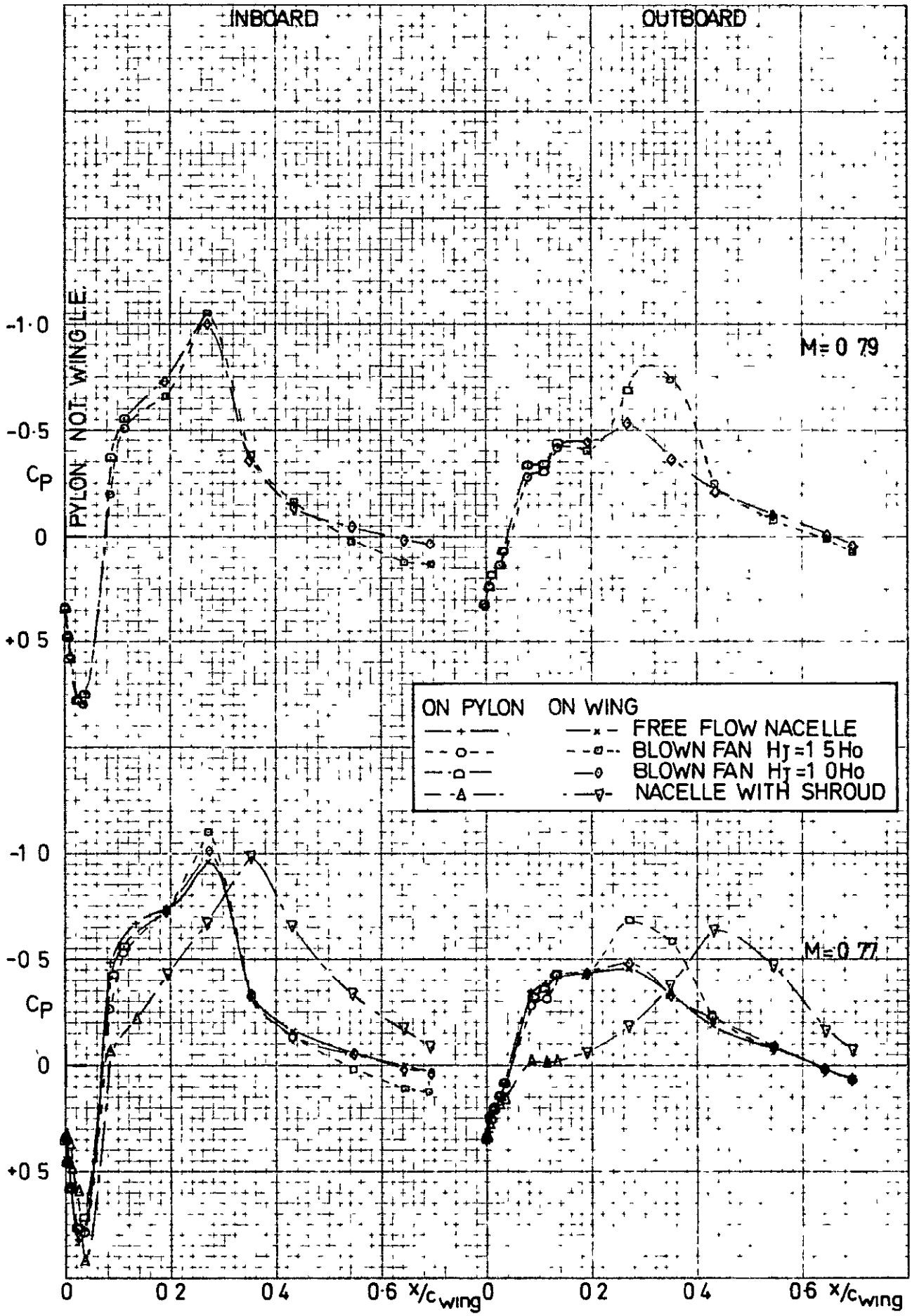

FIG 12b EFFECT OF FAN NOZZLE EXHAUST FLOW AND SHROUD ON PRESSURES AT THE PYLON-WING JUNCTION AT $\alpha_b = 3·5°$

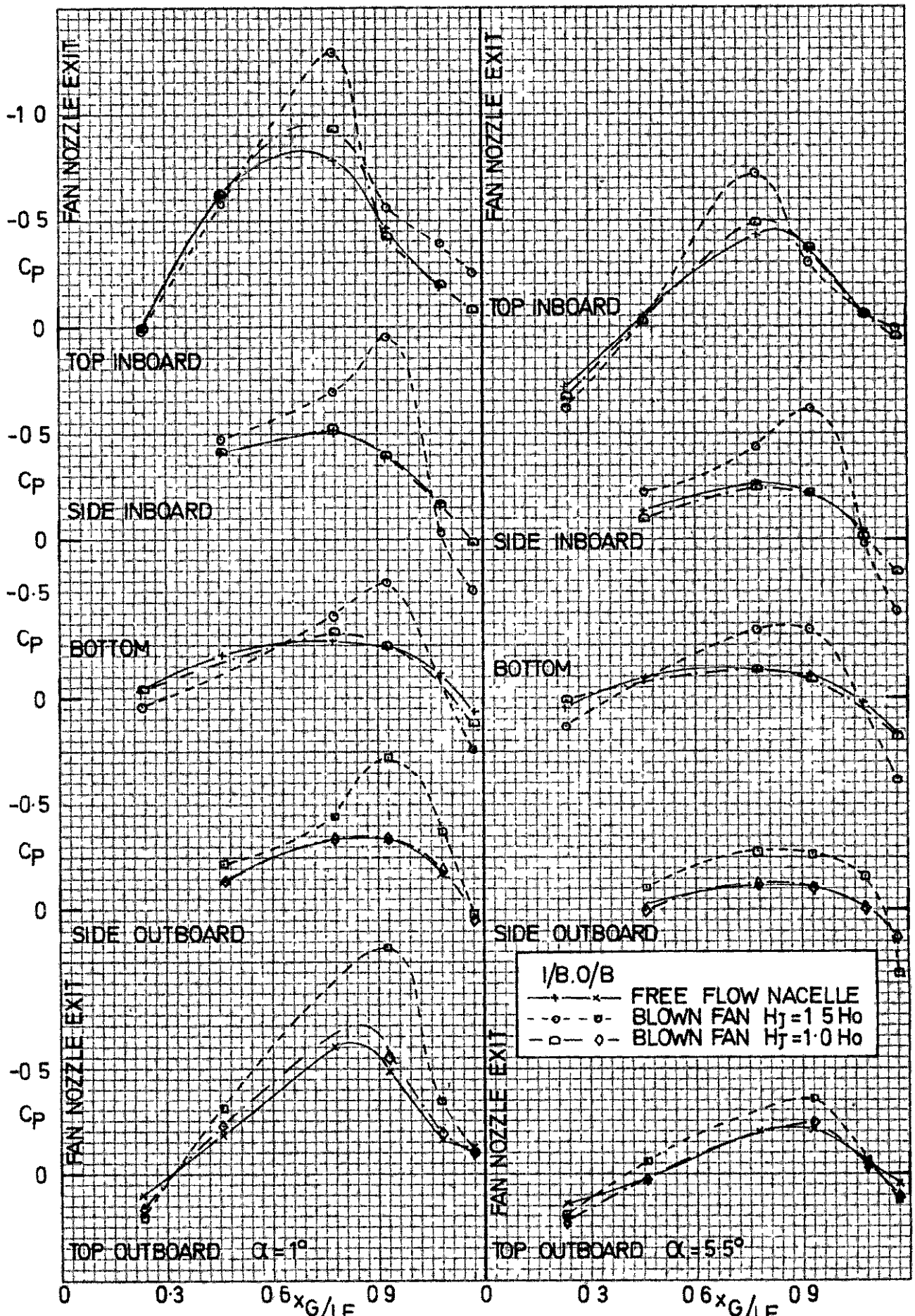

FIG 13 EFFECT OF FAN NOZZLE EXHAUST FLOW ON GAS GENERATOR PRESSURES AT M=0·71

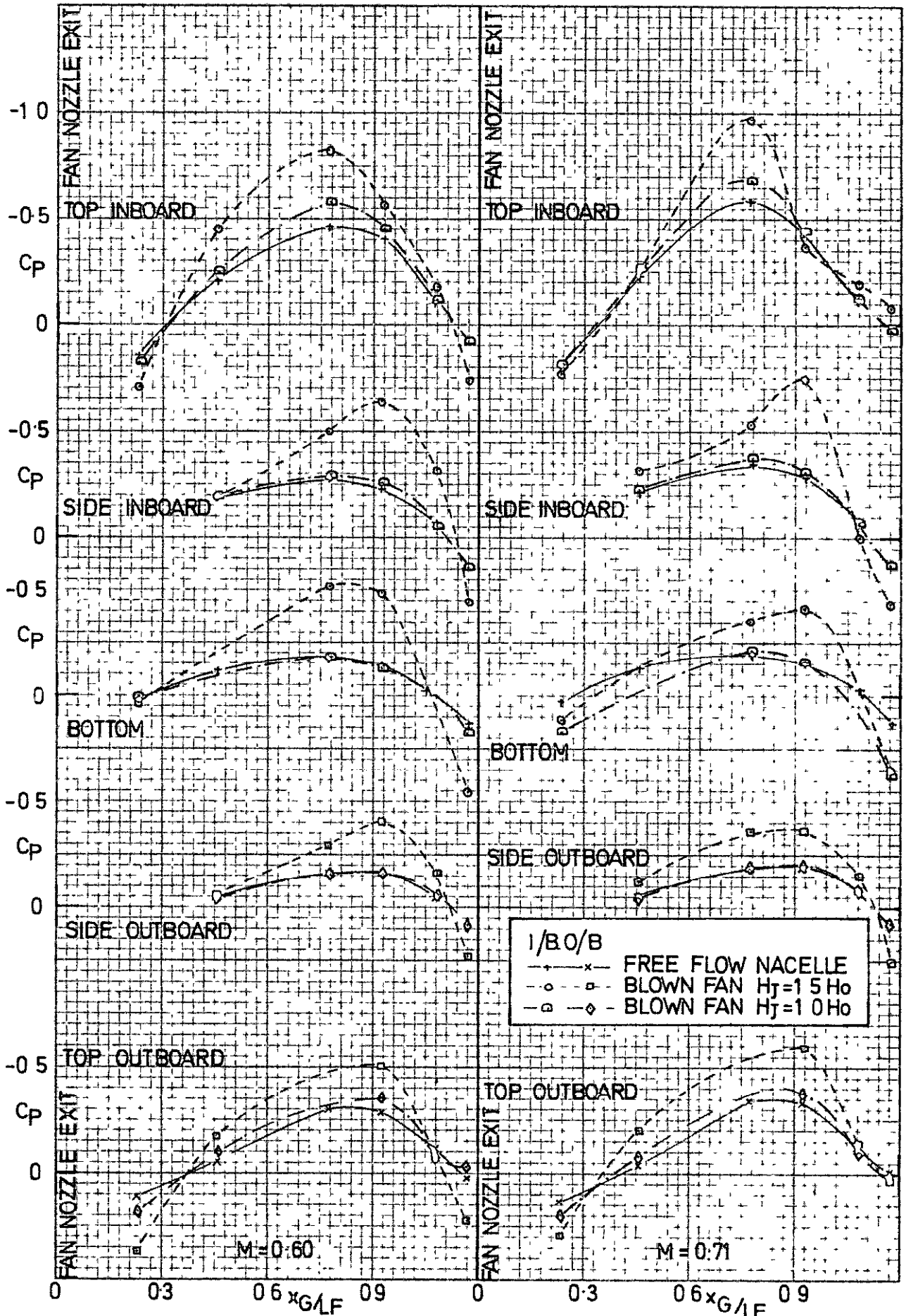

FIG 14a. EFFECT OF FAN NOZZLE EXHAUST FLOW ON GAS GENERATOR PRESSURES AT $\alpha_b = 3{\cdot}5°$

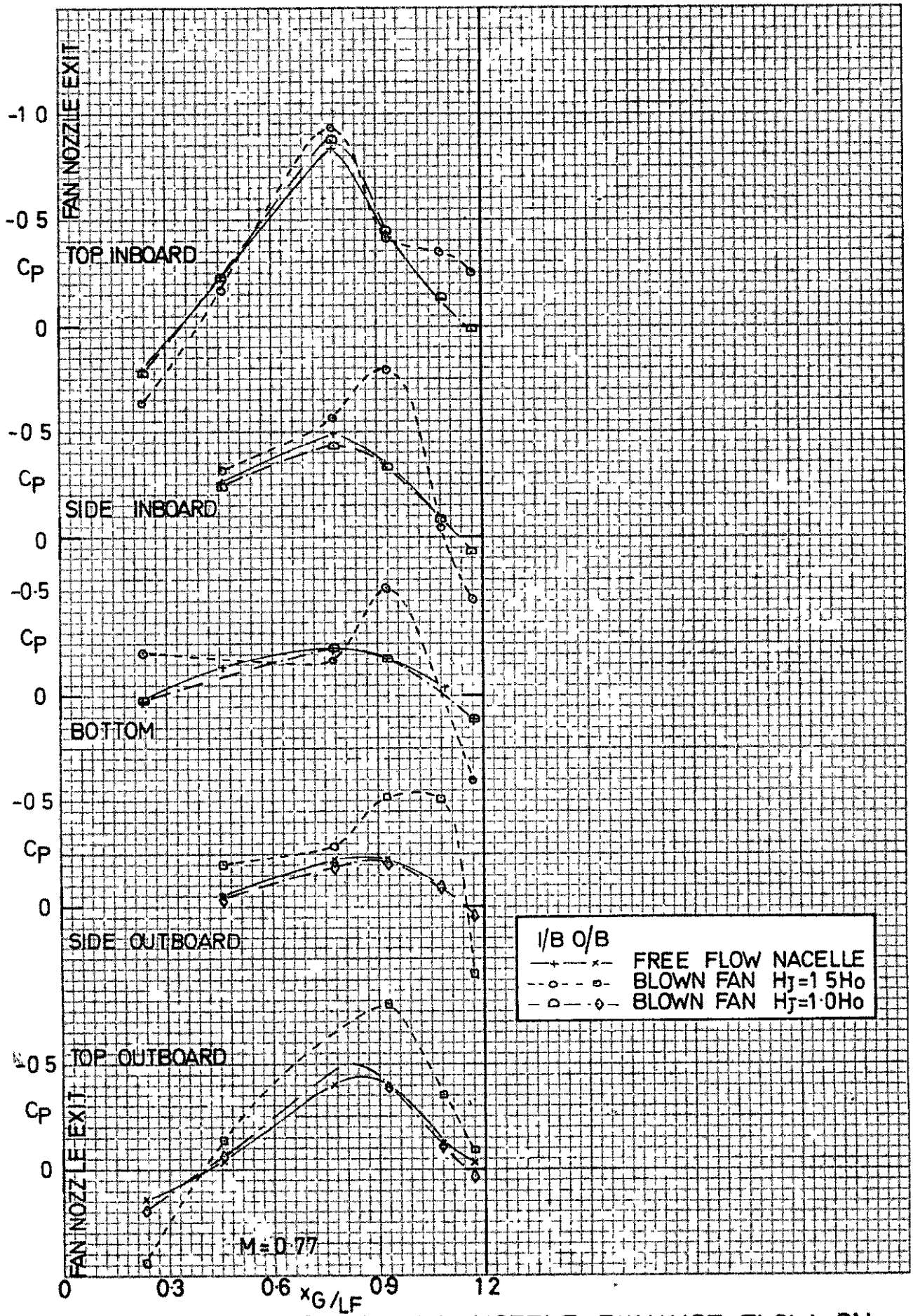

FIG 14b EFFECT OF FAN NOZZLE EXHAUST FLOW ON GAS GENERATOR PRESSURES AT α_D = 3·5°

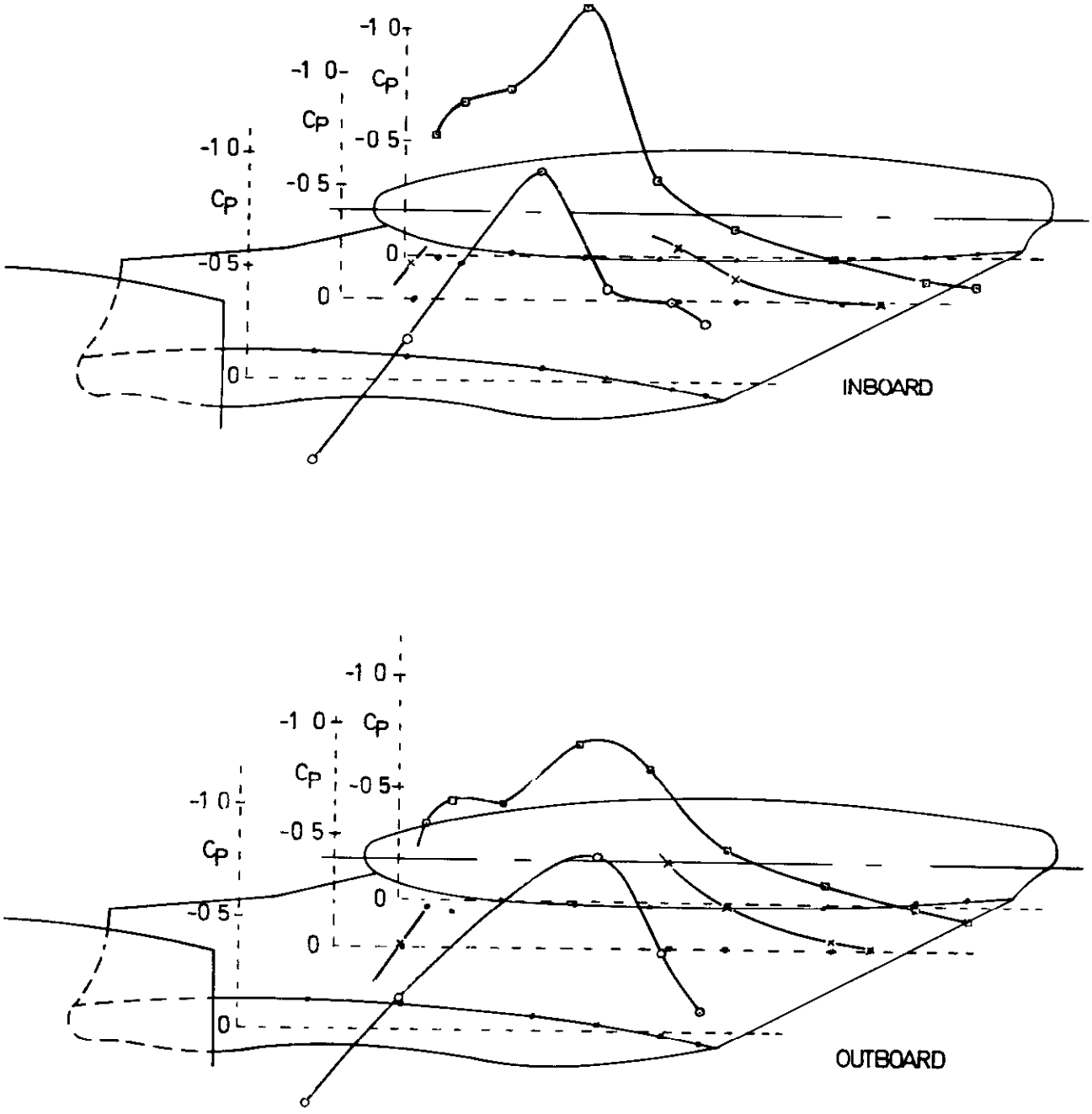

FIG. 15 PYLON PRESSURE DISTRIBUTIONS

$M=0\cdot77 \quad \alpha_D=3\,5° \quad H_J=1\,5H_O$

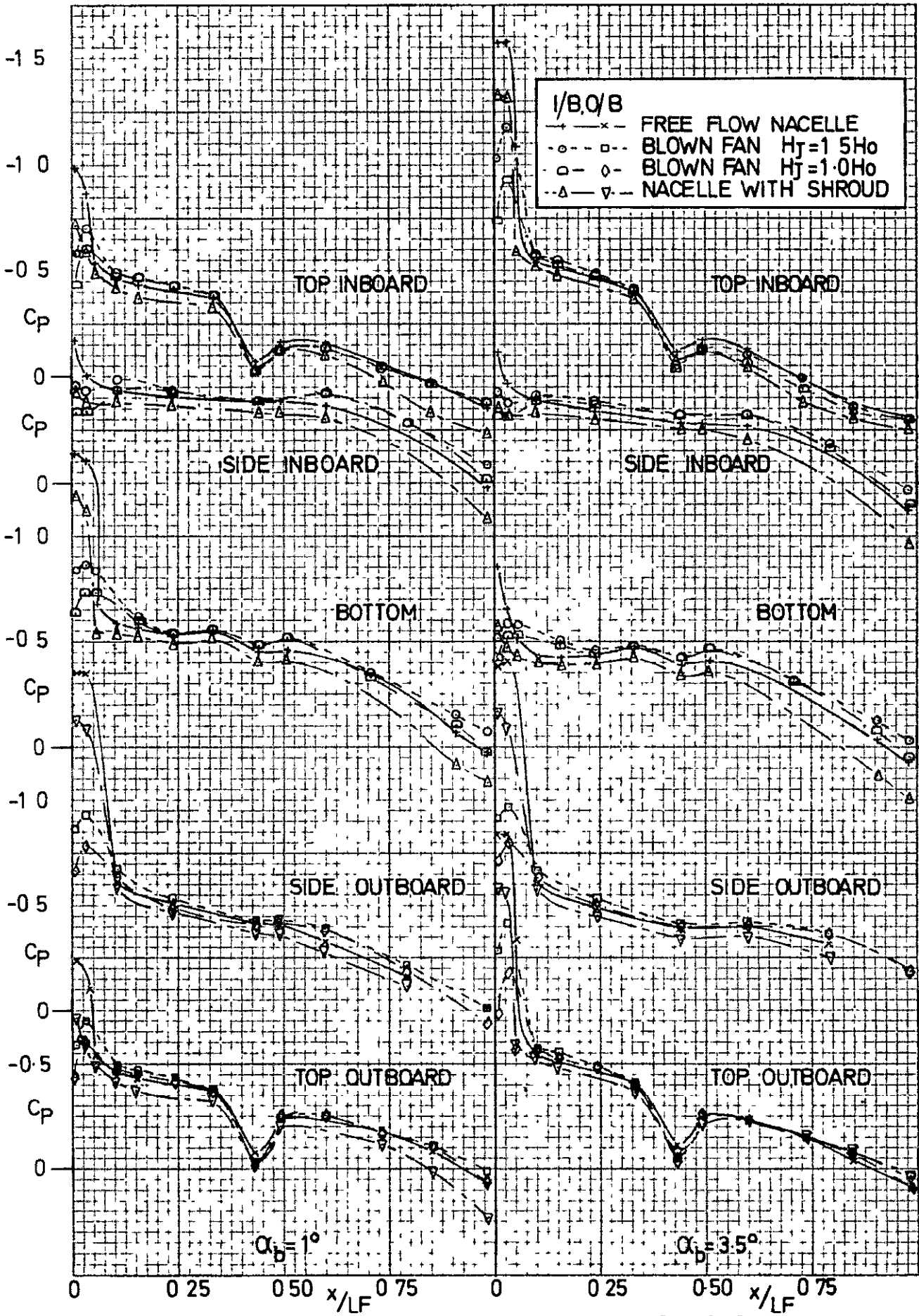

FIG 16a EFFECT OF FAN NOZZLE EXHAUST FLOW AND SHROUD ON FAN COWL PRESSURES AT M=0·71

FIG 16b

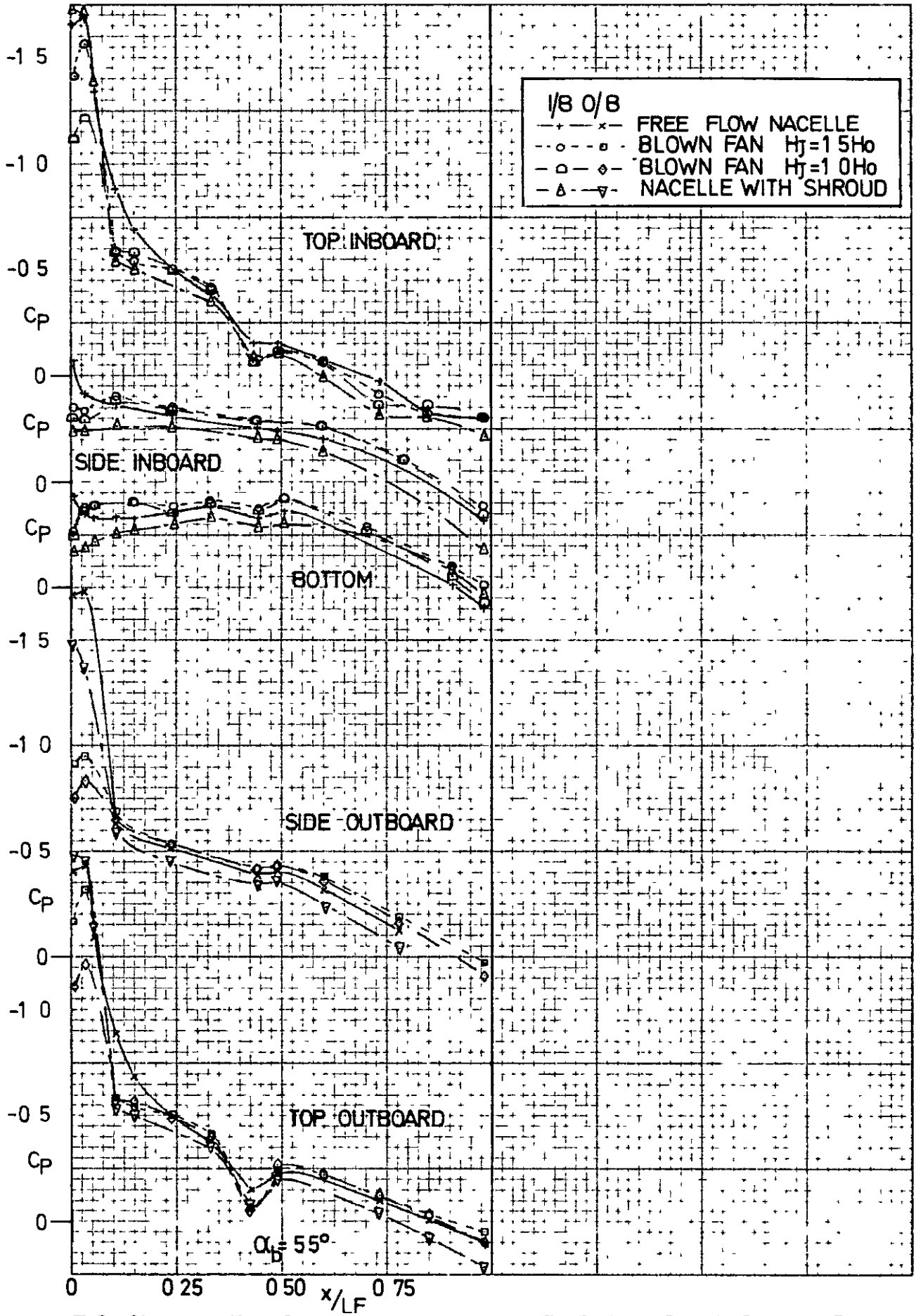

FIG 16b. EFFECT OF FAN NOZZLE EXHAUST FLOW AND SHROUD ON FAN COWL PRESSURES AT M=0·71

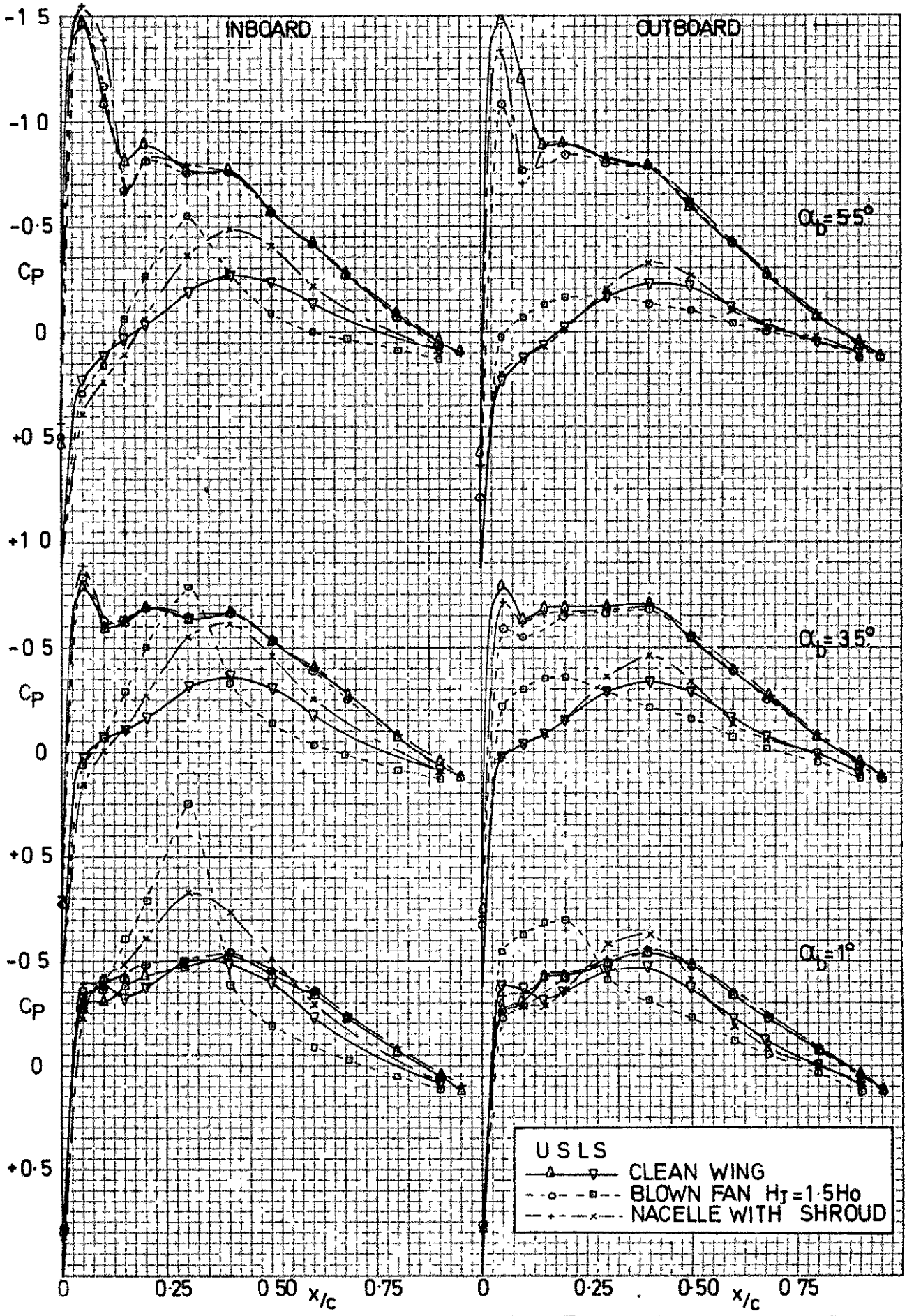

FIG 17. EFFECT OF FAN NOZZLE EXHAUST FLOW AND SHROUD ON WING PRESSURES AT M=0·71

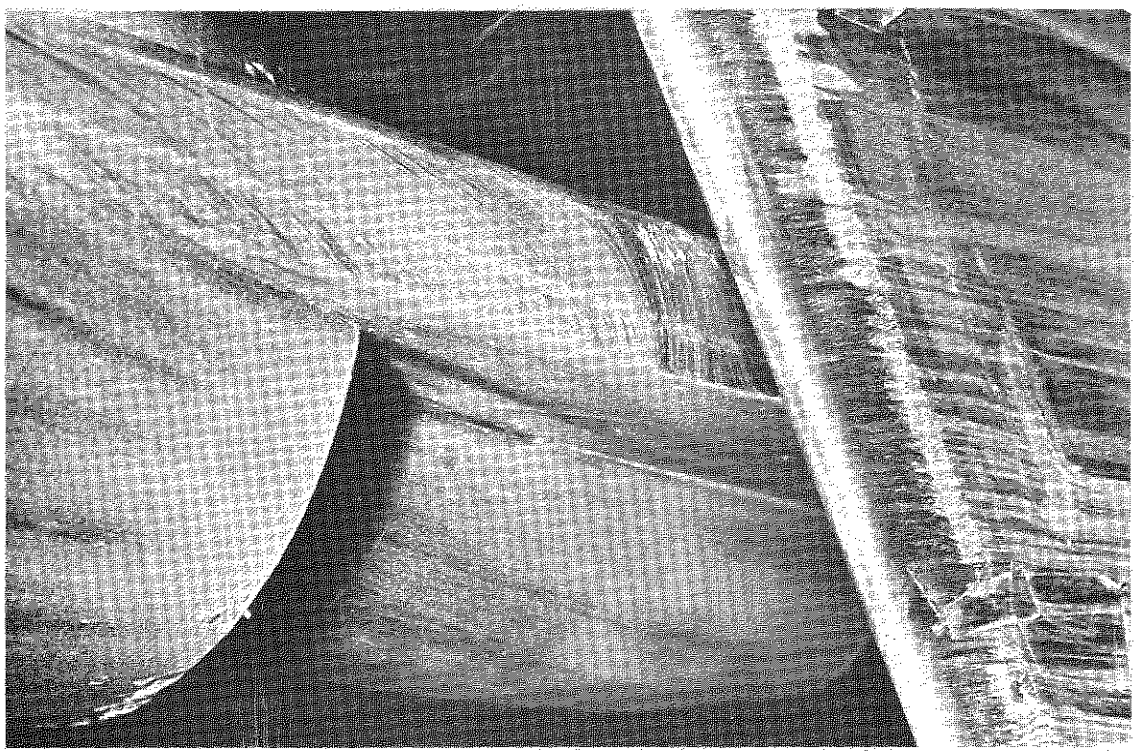

PLATE 1A ORIGINAL PYLON M=0·71 α_b=5·0°

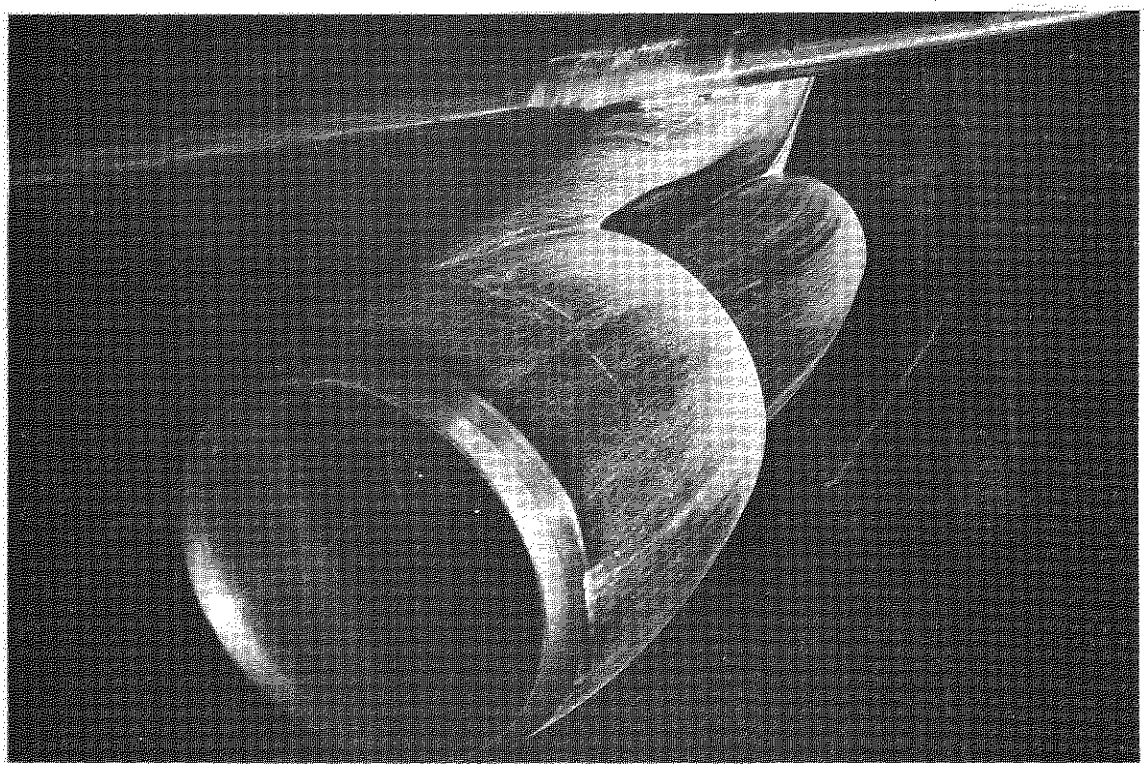

PLATE 1B REVISED PYLON M=0·71 α_b=2·9°

PLATE 1 FLOW ON OUTBOARD SIDE OF PYLON LEADING EDGE – FREE FLOW NACELLE.

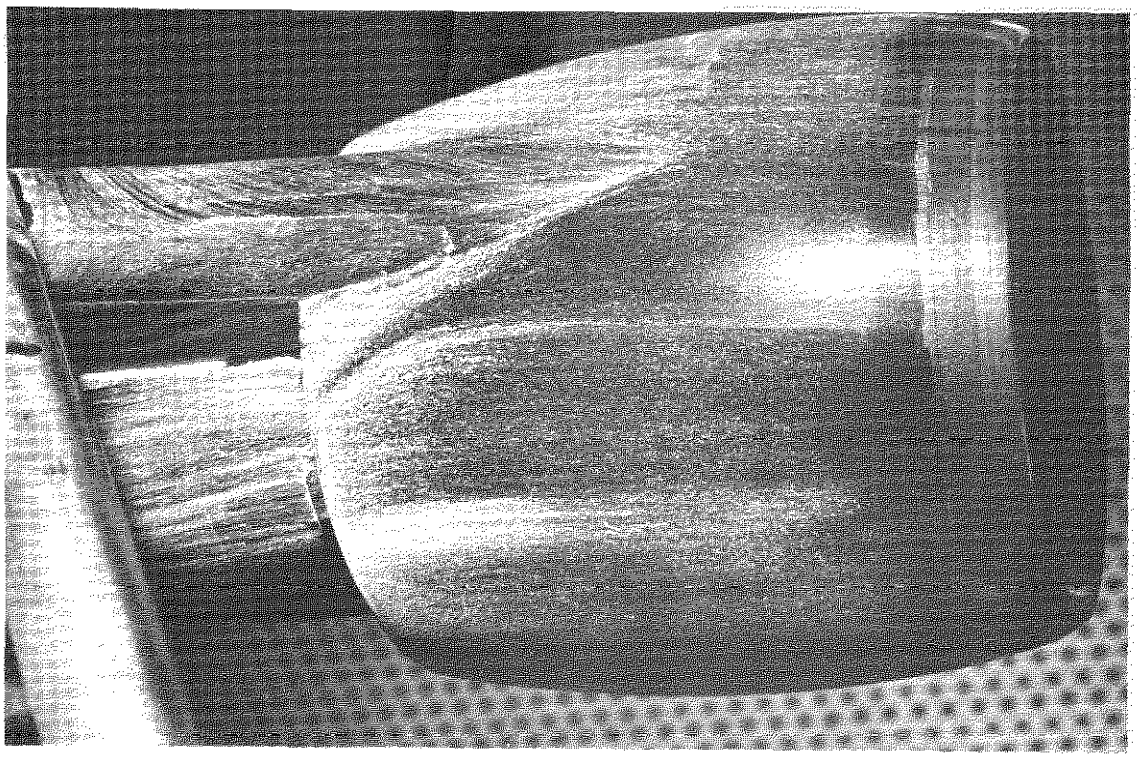

PLATE 2^{A} M = 0·71 α_b = 2·9°

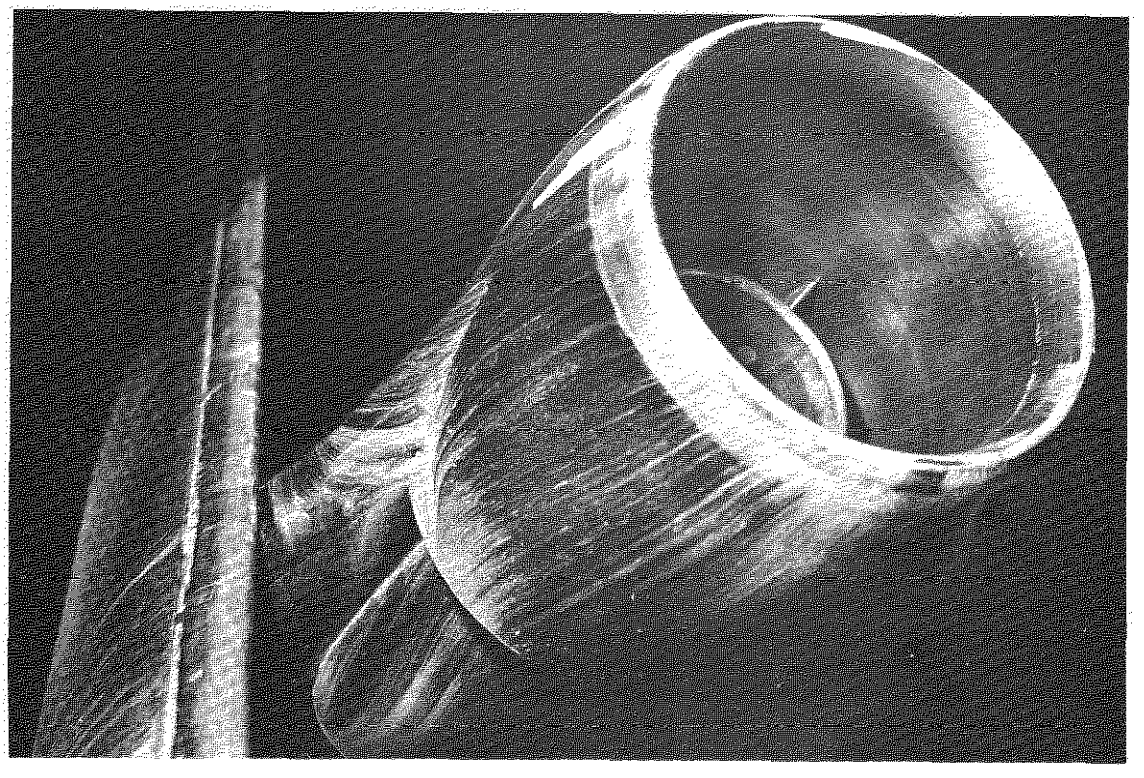

PLATE 2^{B} M = 0·71 α_b = 5·0°

PLATE 2 FLOW ON INBOARD SIDE OF PYLON LEADING EDGE — FREE FLOW NACELLE.

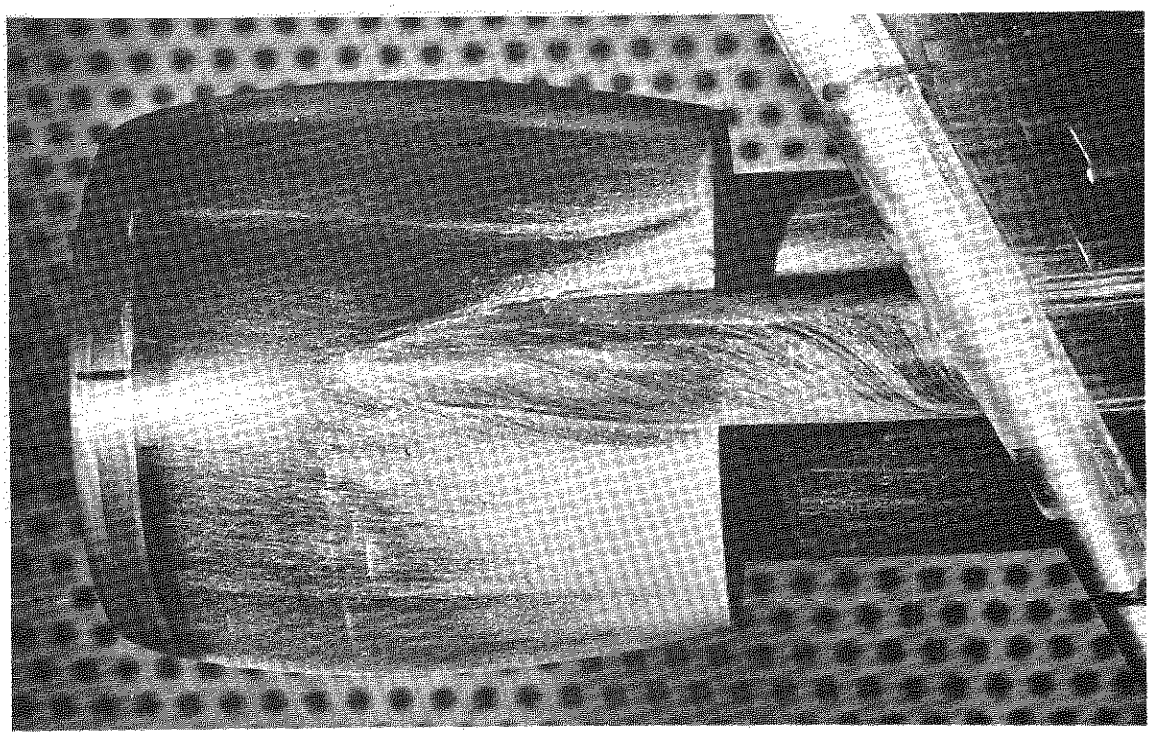

PLATE 3A M=0·71 α_b=2·9°

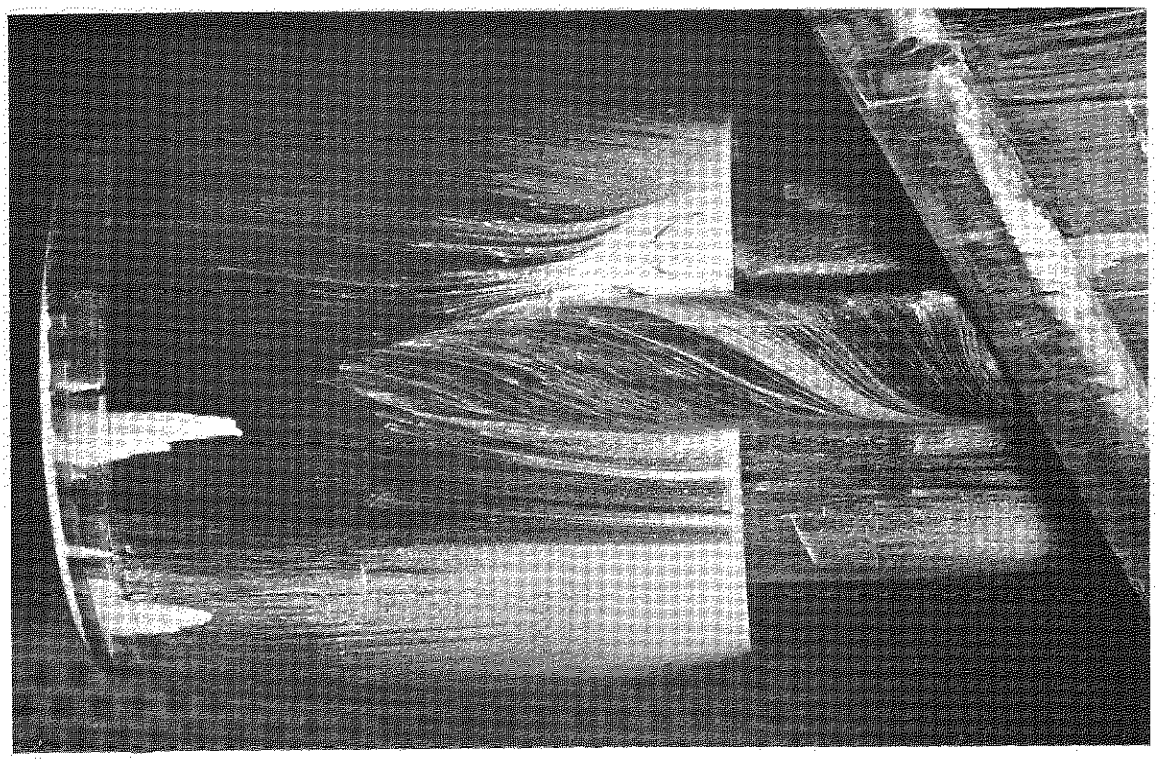

PLATE 3B M=0·71 α_b=5·0°

PLATE 3. FLOW ON UPPER SIDE OF FAN COWL - FREE FLOW NACELLE.

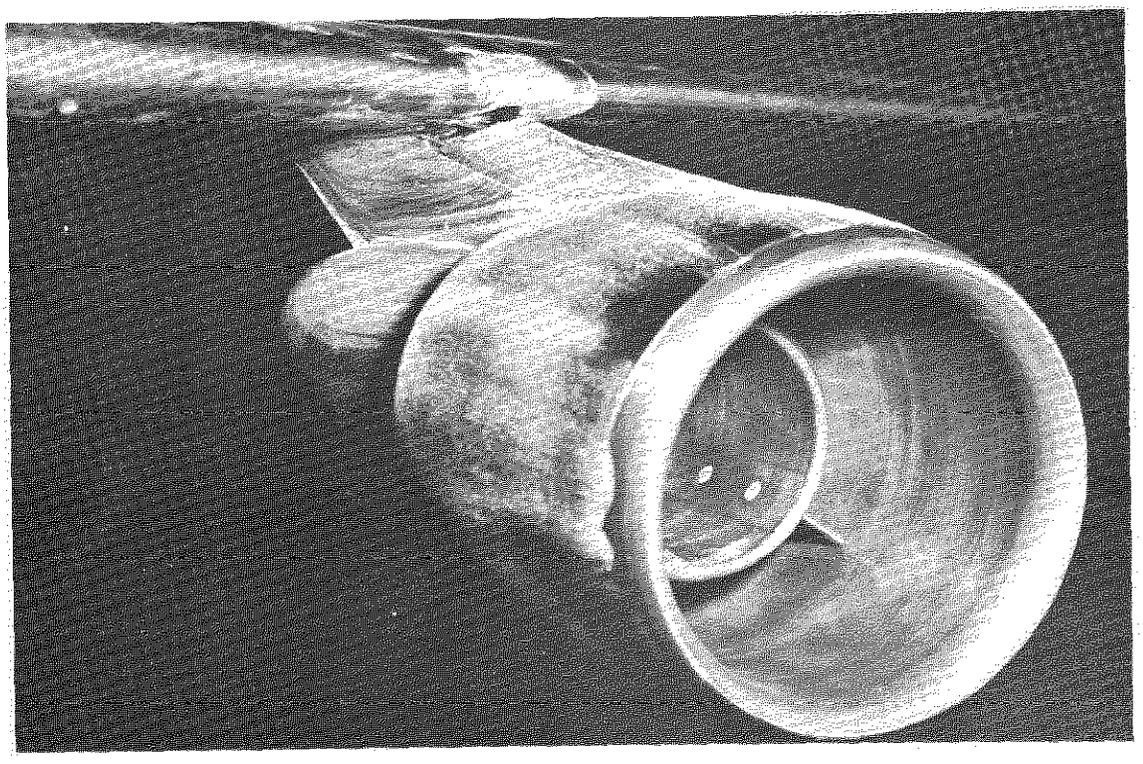

PLATE 4^{A} INBOARD M = 0·71 α_b = 2·9°

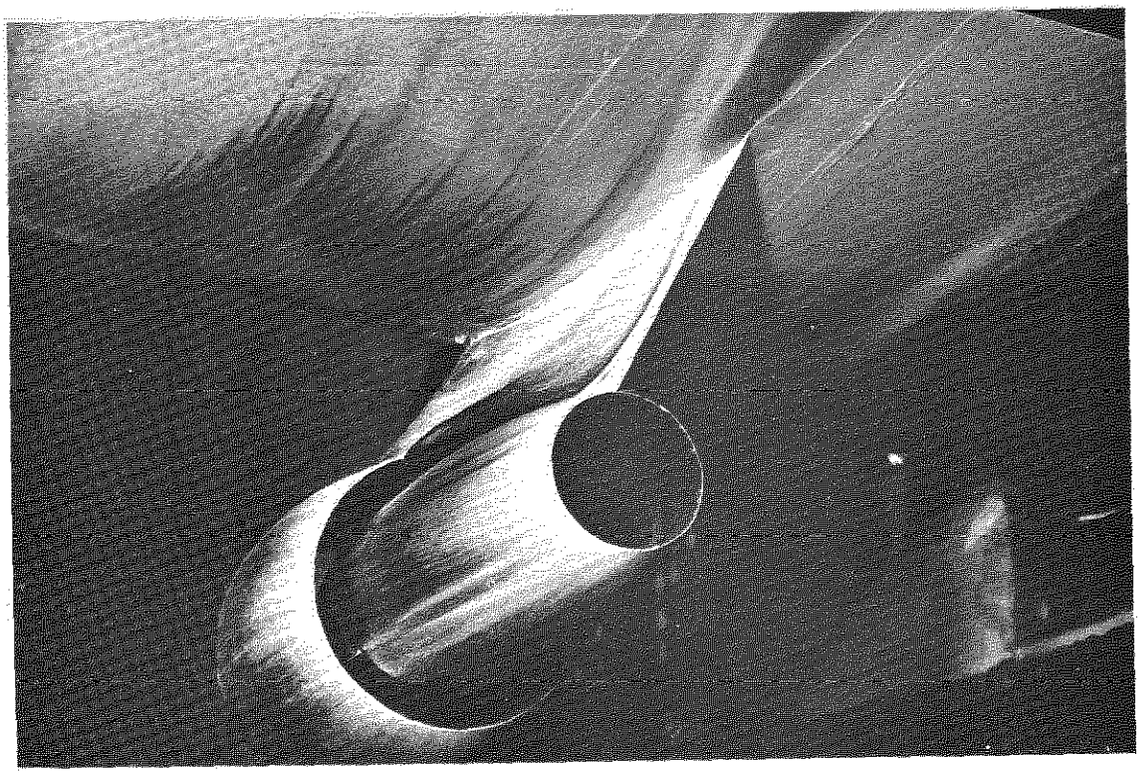

PLATE 4^{B} OUTBOARD M = 0·71 α_b = 2·9°

PLATE 4. FLOW ON PYLON – FREE FLOW NACELLE.

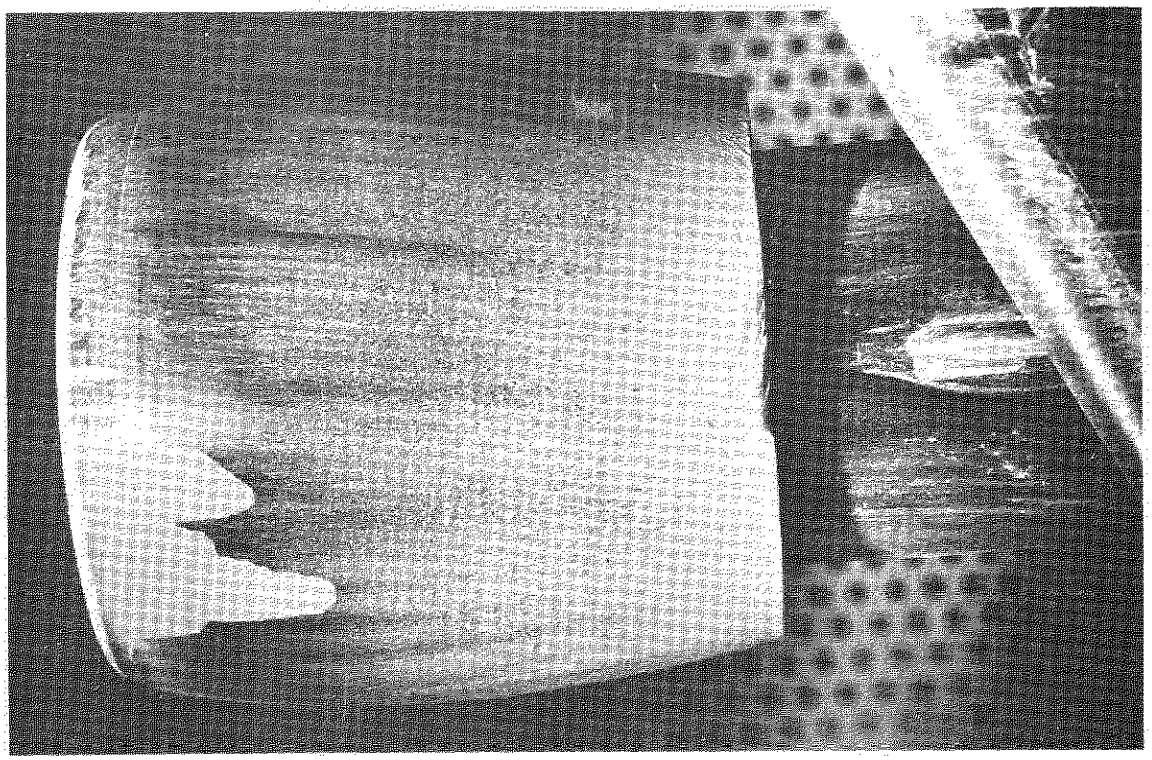

PLATE 5 MINIMUM PYLON – FLOW ON UPPER SIDE OF FAN COWL. $M = 0 \cdot 71$ $\alpha_b = 5 \cdot 0°$

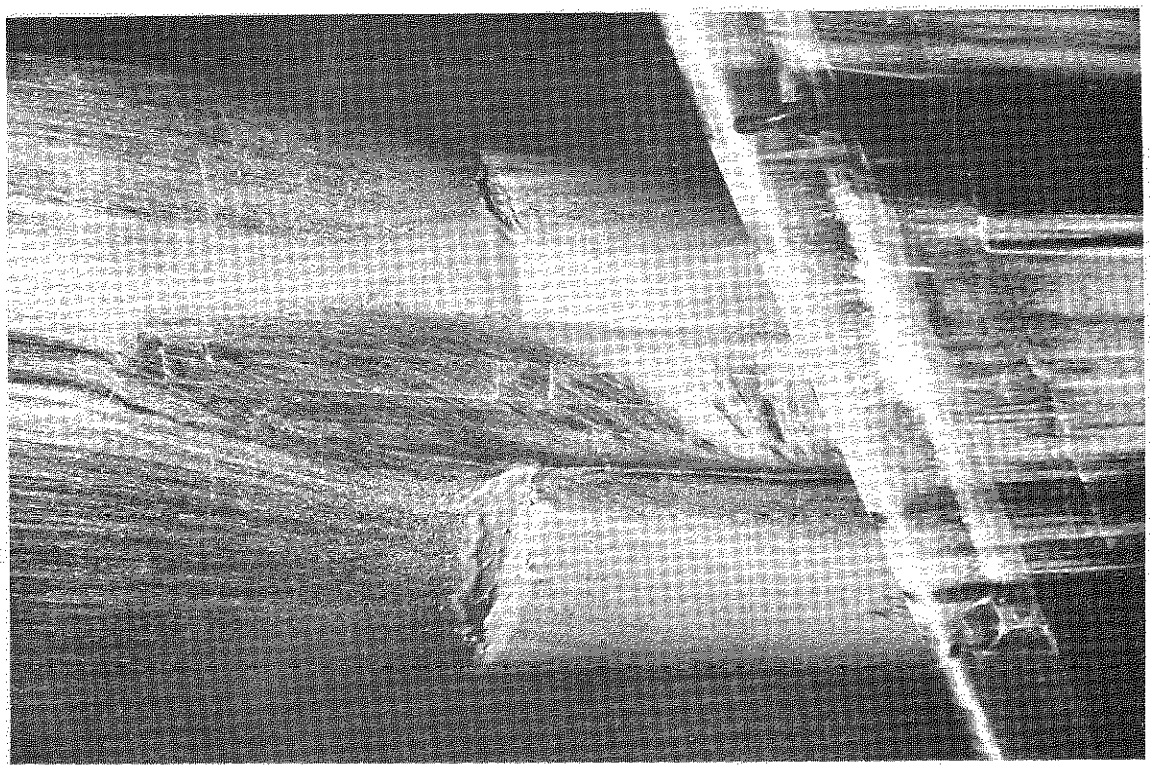

PLATE 6 SHROUDED NACELLE – FLOW ON UPPER SIDE OF FAN COWL $M = 0 \cdot 71$ $\alpha_b = 2 \cdot 9°$

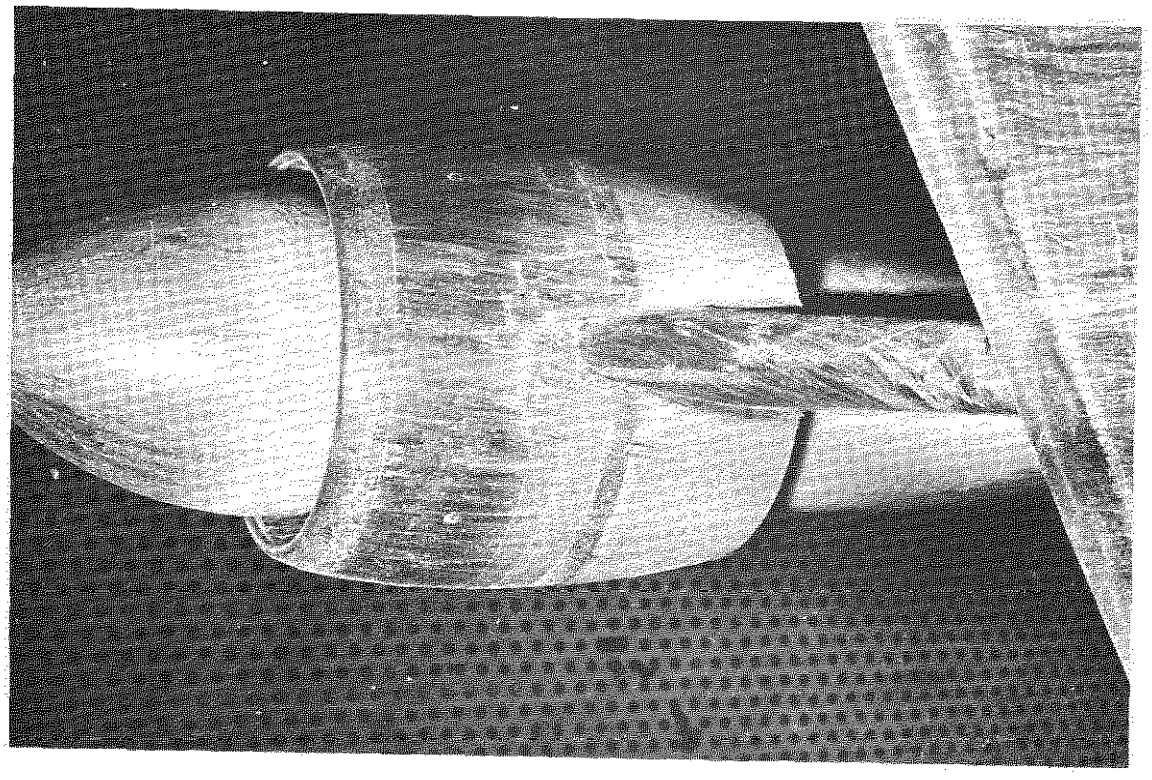

PLATE 7A FLOW ON UPPER SIDE OF FAN COWL M = 0·71 $\alpha_b = 5{\cdot}1°$

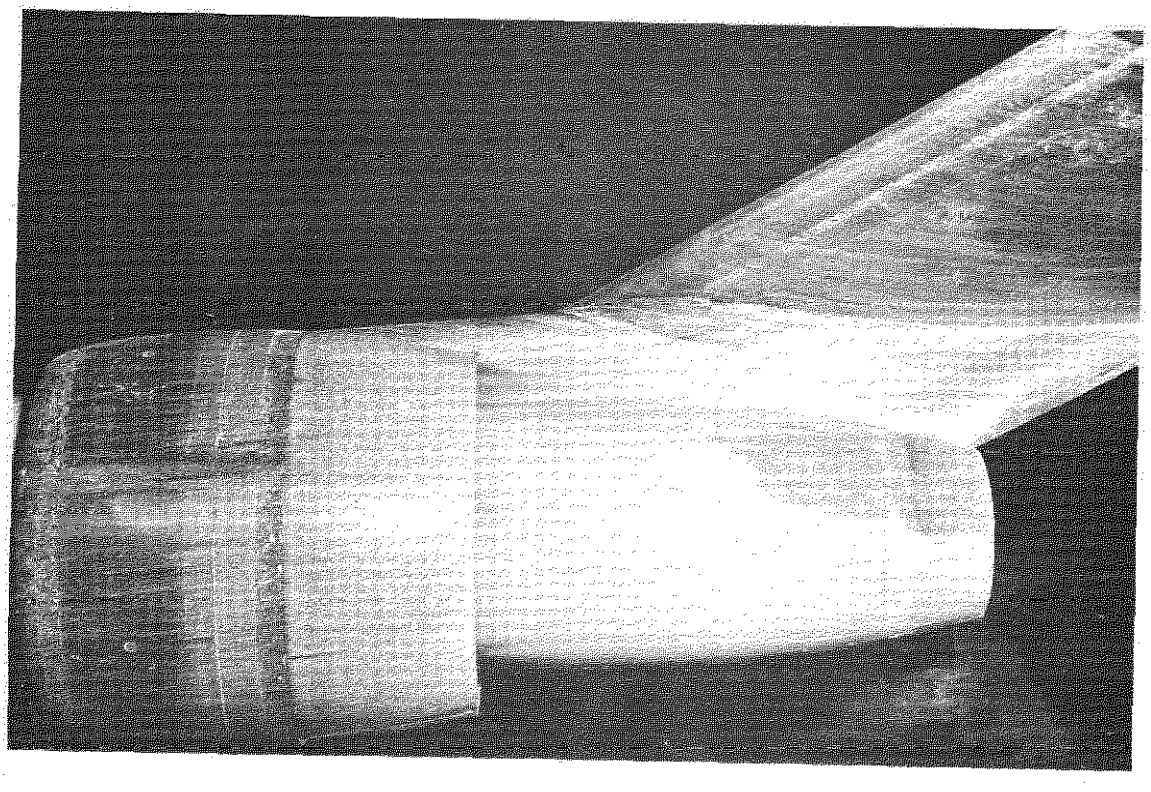

PLATE 7B FLOW ON OUTBOARD SIDE OF NACELLE AND PYLON M = 0·71 $\alpha_{fF} = 5{\cdot}1°$

PLATE 7 FLOW ON BLOWN NACELLE AT M = 0·71 $H_J = 1{\cdot}5\,H_o$.

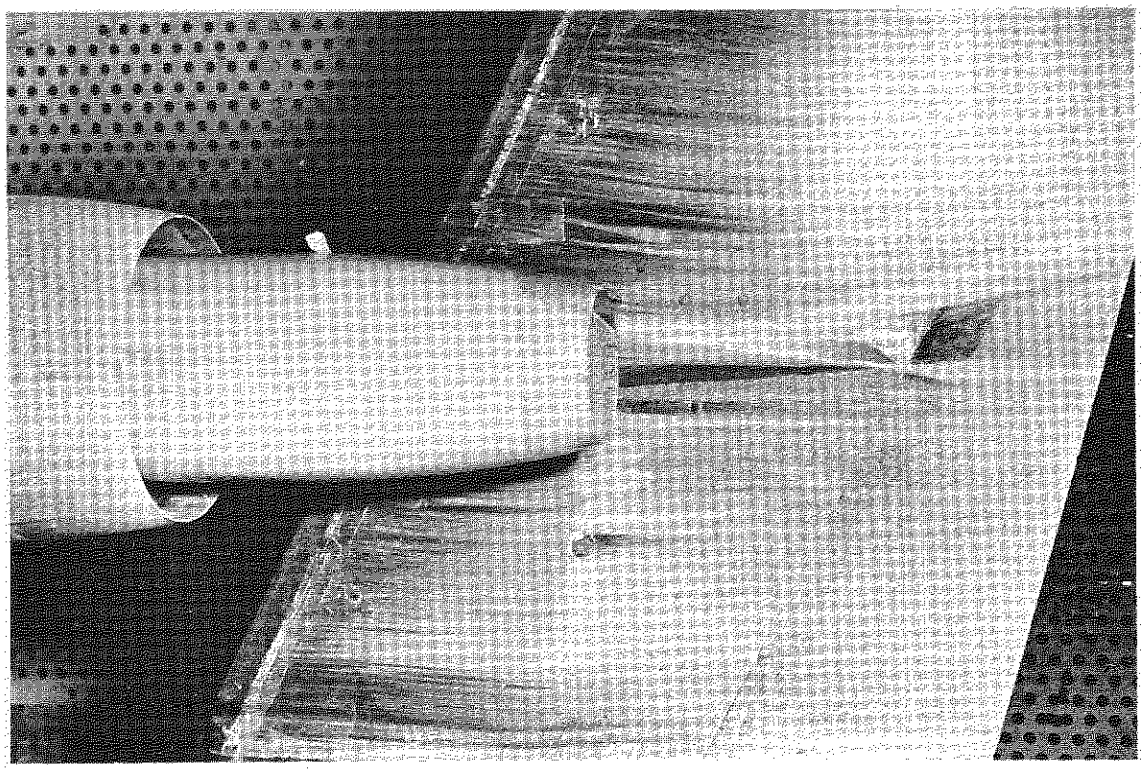

PLATE 8 FLOW ON WING LOWER SURFACE AT HIGH M
- BLOWN NACELLE $M = 0{\cdot}77$ $\alpha_b = 3{\cdot}5°$

Printed and published by
HER MAJESTY'S STATIONERY OFFICE

To be purchased from
49 High Holborn, London WC1
13a Castle Street, Edinburgh EH2 3AR
109 St Mary Street, Cardiff CF1 1JW
Brazennose Street, Manchester M60 8AS
50 Fairfax Street, Bristol BS1 3DE
258 Broad Street, Birmingham 1
7 Linenhall Street, Belfast BT2 8AY
or through any bookseller

Printed in England

C.P. No. 1111

SBN 11 470351 5